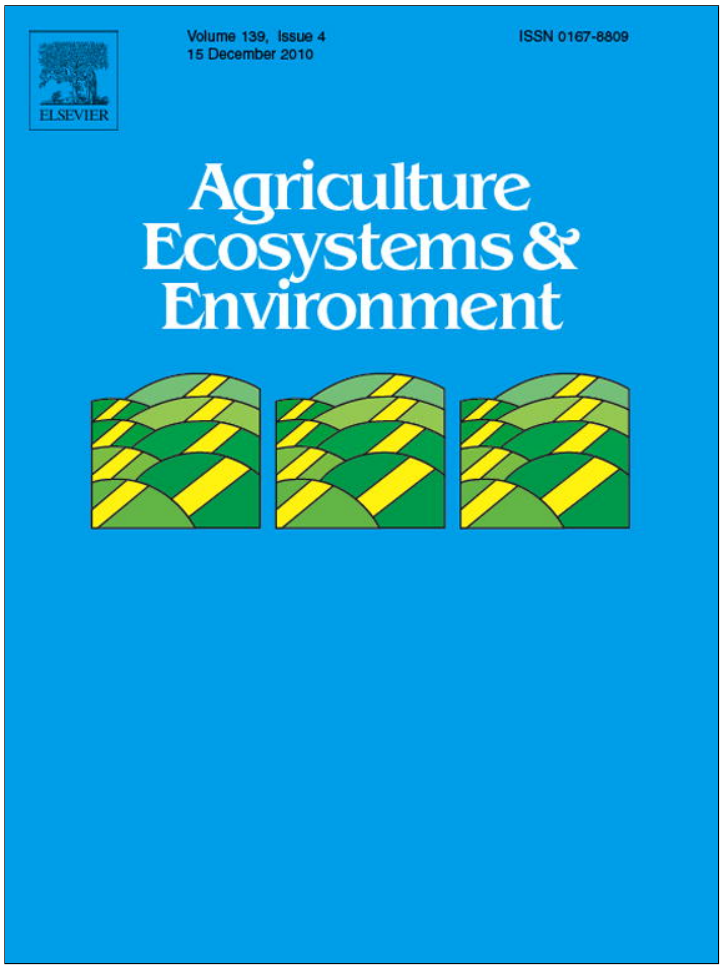

(This is a sample cover image for this issue. The actual cover is not yet available at this time.)

Agriculture, Ecosystems and Environment 150 (2012) 1–18

Contents lists available at SciVerse ScienceDirect

Agriculture, Ecosystems and Environment

journal homepage: www.elsevier.com/locate/agee

Greenhouse gas (CO_2, CH_4, H_2O) fluxes from drained and flooded agricultural peatlands in the Sacramento-San Joaquin Delta

Jaclyn A. Hatala[a,*], Matteo Detto[a,b], Oliver Sonnentag[a,c], Steven J. Deverel[d], Joseph Verfaillie[a], Dennis D. Baldocchi[a]

[a] Ecosystem Science Division, Department of Environmental Science, Policy and Management, University of California 130, Mulford Hall #3114, Berkeley, CA 94720, USA
[b] Smithsonian Tropical Research Institute, Panama City, Panama
[c] Département de Géographie, Université de Montréal, Montreal, Canada
[d] Hydrofocus, Inc., Davis, CA, USA

ARTICLE INFO

Article history:
Received 14 October 2011
Received in revised form 6 January 2012
Accepted 8 January 2012

Keywords:
Carbon flux
Evaporation
Rice
Peatland
Eddy covariance
Evaporation

ABSTRACT

The Sacramento-San Joaquin Delta in California was drained and converted to agriculture more than a century ago, and since then has experienced extreme rates of soil subsidence from peat oxidation. To reverse subsidence and capture carbon there is increasing interest in converting drained agricultural land-use types to flooded conditions. Rice agriculture is proposed as a flooded land-use type with CO_2 sequestration potential for this region. We conducted two years of simultaneous eddy covariance measurements at a conventional drained and grazed degraded peatland and a newly converted rice paddy to evaluate the impact of drained to flooded land-use change on CO_2, CH_4, and evaporation fluxes.

We found that the grazed degraded peatland emitted 175–299 g-C m^{-2} yr^{-1} as CO_2 and 3.3 g-C m^{-2} yr^{-1} as CH_4, while the rice paddy sequestered 84–283 g-C m^{-2} yr^{-1} of CO_2 from the atmosphere and released 2.5–6.6 g-C m^{-2} yr^{-1} as CH_4. The rice paddy evaporated 45–95% more water than the grazed degraded peatland. Annual photosynthesis was similar between sites, but flooding at the rice paddy inhibited ecosystem respiration, making it a net CO_2 sink. The rice paddy had reduced rates of soil subsidence due to oxidation compared with the drained peatland, but did not completely reverse subsidence.

1. Introduction

Draining peatlands for agricultural cultivation results in some of the fastest rates and largest magnitudes of carbon loss attributable to land-use change. Nevertheless, peatland drainage is practiced around the world due to the high economic benefit of fertile soil. As a direct consequence of anthropogenic manipulation for agriculture and settlement, much of the land within the world's largest river deltas is sinking due to soil loss and compaction following drainage (Syvitski et al., 2009). Large river basins such as the Changjiang (China), Mississippi (USA), and Ganges-Brahmaputra (India, Bangladesh) are now identified as "natural recorders" of upstream land-use decisions (Bianchi and Allison, 2009), as around the world the demand for agricultural production has made croplands and pastures one of the largest terrestrial biomes (Ramankutty et al., 2008). Land-use conversion from natural ecosystems to agricultural production has consequences for global biogeochemical cycling and climate through changes to carbon dynamics and the energy exchange between the land and atmosphere (Foley et al., 2005).

The Sacramento-San Joaquin Delta (hereafter, the Delta) in California is yet another example of a delta peatland that has undergone rapid environmental change, with irreversible alteration of the carbon cycle due to drainage, conversion to agriculture, and subsequently large rates of soil subsidence (Weir, 1950; Armentano, 1980; Deverel and Leighton, 2010). The pre-reclamation Delta peatlands encompassed an area about 2125 km^2 inland of San Francisco Bay (Thompson, 1957) that existed as a network of saltwater and freshwater marshes for nearly 7000 years following the last Holocene glaciation (Shlemon and Begg, 1975; Drexler et al., 2009a). High rates of primary productivity, low rates of decomposition, and gradual sea-level rise during the Delta's long period of inundation formed a layer of peat soil over 15 m thick (Shlemon and Begg, 1975; Drexler et al., 2007). However, the Delta islands were drained during the latter half of the 19th century and beginning of the 20th century, dramatically reversing the rate of carbon accumulation (Thompson, 1957; Canuel et al., 2009). Drainage of the Delta created a network of "islands" that maintain an artificially low water table through an extensive and fragile 1700 km levee system and continual island drainage (Mount and Twiss, 2005). Agricultural cultivation since drainage has resulted in extreme rates of soil subsidence due to peat compaction and oxidation, and the land surface of Delta islands is now on average 5–8 m below sea

* Corresponding author. Tel.: +1 510 642 9048, fax: +1 510 643 5098.
E-mail address: jhatala@berkeley.edu (J.A. Hatala).

0167-8809/$ – see front matter © 2012 Elsevier B.V. All rights reserved.
doi:10.1016/j.agee.2012.01.009

level (Drexler et al., 2009b; Deverel and Leighton, 2010). The total amount of carbon lost from the Delta since drainage has been estimated at 0.5 petagrams of CO_2 (Crooks, 2009), and Deverel and Leighton (2010) estimated that annual median CO_2 loss from Delta islands is about 17,000 g-C ha^{-1}.

Decreasing the rate of peat oxidation in the Delta is the key to slowing soil subsidence and turning drained Delta ecosystems from net carbon sources to sinks. Choosing management practices that preserve soil carbon, especially for non-growing season fluxes, has been shown to effectively decrease the net emission of CO_2 from agricultural ecosystems (Miller et al., 2000, 2008; Smith et al., 2007; Jans et al., 2010). The conversion from conventional drained agriculture to flooded systems like rice paddies has been identified as a potential management intervention for the Delta that could inhibit further peat oxidation (Lund et al., 2007). Miller et al. (2000) demonstrated that wetlands flooded from early spring through midsummer resulted in a net carbon gain. Rice growers use a similar water management practice, flooding rice fields during the warmest months when soil oxidation rates are highest, so rice is hypothesized to be a viable crop for stopping subsidence. The flooded status of rice paddy soils impedes peat oxidation by physically limiting the transport of oxygen into the soil profile, a requirement for most microbial metabolisms. Thus, rates of ecosystem respiration are significantly lower in rice paddies than in other agricultural systems (Eugster et al., 2010). Previous work has indicated that raising the water table in peat soils can significantly decrease CO_2 production and even reverse net ecosystem carbon loss (Hendriks et al., 2007; Waddington et al., 2010; Worrall et al., 2010).

However, managing land for CO_2 capture is likely to change the fluxes of other greenhouse gases from the ecosystem, in addition to altering the energy balance of the landscape (Pielke et al., 2002). While there is good evidence that flooding for rice will help to stop the net loss of CO_2 from peat oxidation, the conversion from drained to flooded soils creates ideal conditions for the anaerobic microbial production of CH_4, a greenhouse gas with 25 times the radiative forcing capacity of CO_2 over a 100-year time frame (Forster et al., 2007). In addition to potentially increasing CH_4 emissions, the conversion from drained to flooded conditions within the Delta's Mediterranean climate might also increase evaporation, as free standing water is more directly exposed to the atmosphere. Increased loss of water flowing through the Delta could create further tension within California's long-standing water wars, as the Delta is the nexus of drinking water distribution for 23 million Californians and nearly all the state's irrigation water (Schwarzenegger et al., 2008). However, conversion of Delta islands to rice might limit future subsidence and reduce the rate of increasing levee fragility by reducing the hydraulic gradient from channels onto islands and stopping or reducing ever-increasing hydraulic forces on levees due to subsidence. To address the short-term consequences and trade-offs of conversion from drained to flooded agriculture on carbon, water, and energy exchange, this study examined differences in continuous CO_2 and CH_4 fluxes as well as the evaporation and the energy balance between a drained and grazed degraded peatland and a recently-converted flooded rice paddy in the Delta over two years (Fig. 1).

From April 2009 to April 2011, we measured the fluxes of CO_2, CH_4, H_2O, and energy at the drained and grazed degraded peatland and flooded rice paddy using the eddy covariance method (Baldocchi et al., 1988), and aggregated these fluxes over two years to calculate net annual budgets for April 2009–April 2010 and April 2010–April 2011. We measured the terrestrial carbon balance in the Delta as the net budgets of CO_2 (net ecosystem exchange; NEE) and CH_4 flux. CO_2 is captured by plants through photosynthesis (ecosystem photosynthesis; P_{eco}) and represents a sink from the atmosphere, and CO_2 is produced by plant and microbial respiration (ecosystem respiration; R_{eco}) and represents a source to the atmosphere. P_{eco} is expressed as negative and R_{eco} as positive, so that negative NEE respresents net CO_2 uptake and positive NEE represents net CO_2 release. CH_4 is produced as the metabolic end-product of a small group of *Archaea* that exist only in anaerobic conditions, such as flooded soils and ruminant digestive tracts, and this production acts as a source to the atmosphere (Conrad, 2007). In vegetated rice paddies, most CH_4 is transported from the soil where it is produced, through the porous aerenchyma tissue of rice plant to the atmosphere, and most methane is transported by diffusion and ebullition (bubbling) in during the winter months when the rice paddy is fallow (Holzapfel-Pschorn et al., 1986; Schutz et al., 1989). At the grazed degraded peatland, CH_4 is produced within flooded drainage ditches and in zone of saturation in the soil profile (Teh et al., 2011). CH_4 is consumed in the aerobic zone in soils at both sites through the cosmopolitan metabolic pathway of a group of organisms called methanotrophs, which convert CH_4 into CO_2. Although methanotrophs are not a strong sink of atmospheric CH_4, they can consume 48–78% of methane produced at lower depths in upland soils (Teh et al., 2005) and 20–60% of CH_4 produced in rice paddy soils (Tyler et al., 1997) as CH_4 diffuses from the anaerobic zone where it is produced upward through the soil and water profile. The method used to partition NEE into sinks by ecosystem photosynthesis (P_{eco}) and sources through ecosystem respiration (R_{eco}) cannot likewise partition soil CH_4 fluxes into CH_4 production (methanogenesis) and CH_4 consumption (methanotrophy).

The first goal in our analysis was to compare carbon capture in the rice paddy with the drained grazed peatland on an annual timescale. We hypothesized that the grazed degraded peatland would be a larger net source of carbon than the rice paddy, as we expected the drained peat soil at the grazed peatland to have higher rates of R_{eco} and lower rates of P_{eco} than the flooded and productive rice paddy. We also considered the measured CH_4 emissions from each site as carbon losses for this net carbon balance calculation, and expected CH_4 flux from the rice paddy to exceed that from the drained and grazed peatland since the CH_4 produced in the drained soil has a much larger opportunity to be oxidized by microbes into CO_2 as it diffuses through the aerated soil zone to the atmosphere. As we expected the drained peatland to be a larger source of carbon from the ecosystem, we hypothesized that it would have larger rates of subsidence due to soil oxidation than the flooded rice paddy.

Our second goal was to quantify the effects of land-use conversion from drained to flooded soils on the CH_4 budget since it has a higher radiative forcing than CO_2, which can alter the greenhouse gas radiative forcing budget of the ecosystem. Since the flooded paddy soil creates ideal anaerobic conditions for CH_4 production and incorporates fresh biomass into the soil each year through the residual straw left on the field after harvest, we expected the net budget of CH_4 at the rice paddy to exceed that of the grazed degraded peatland (Cicerone et al., 1992). Using the CO_2-equilvalent conversion factor for CH_4 of 25, the hypothesized higher rate of CH_4 production at the rice paddy could transform the ecosystem into a net positive greenhouse gas forcing budget even though it might be a net sink for CO_2 (Forster et al., 2007).

The final goal of our work was to analyze differences between the evaporation budgets at the two sites. We expected that evaporation would be higher at the rice paddy than the grazed degraded peatland since the water surface at the rice paddy is directly exposed to the atmosphere for much of the year. However, we considered that it was possible that evaporation from the grass canopy and shallow water table at the grazed degraded peatland during the winter might exceed that from the fallow but flooded rice paddy due to the higher canopy conductance of rough vegetation when compared with a flat water surface. Together, these hypotheses provide important information about the short-term impacts and significant environmental trade-offs of land-use

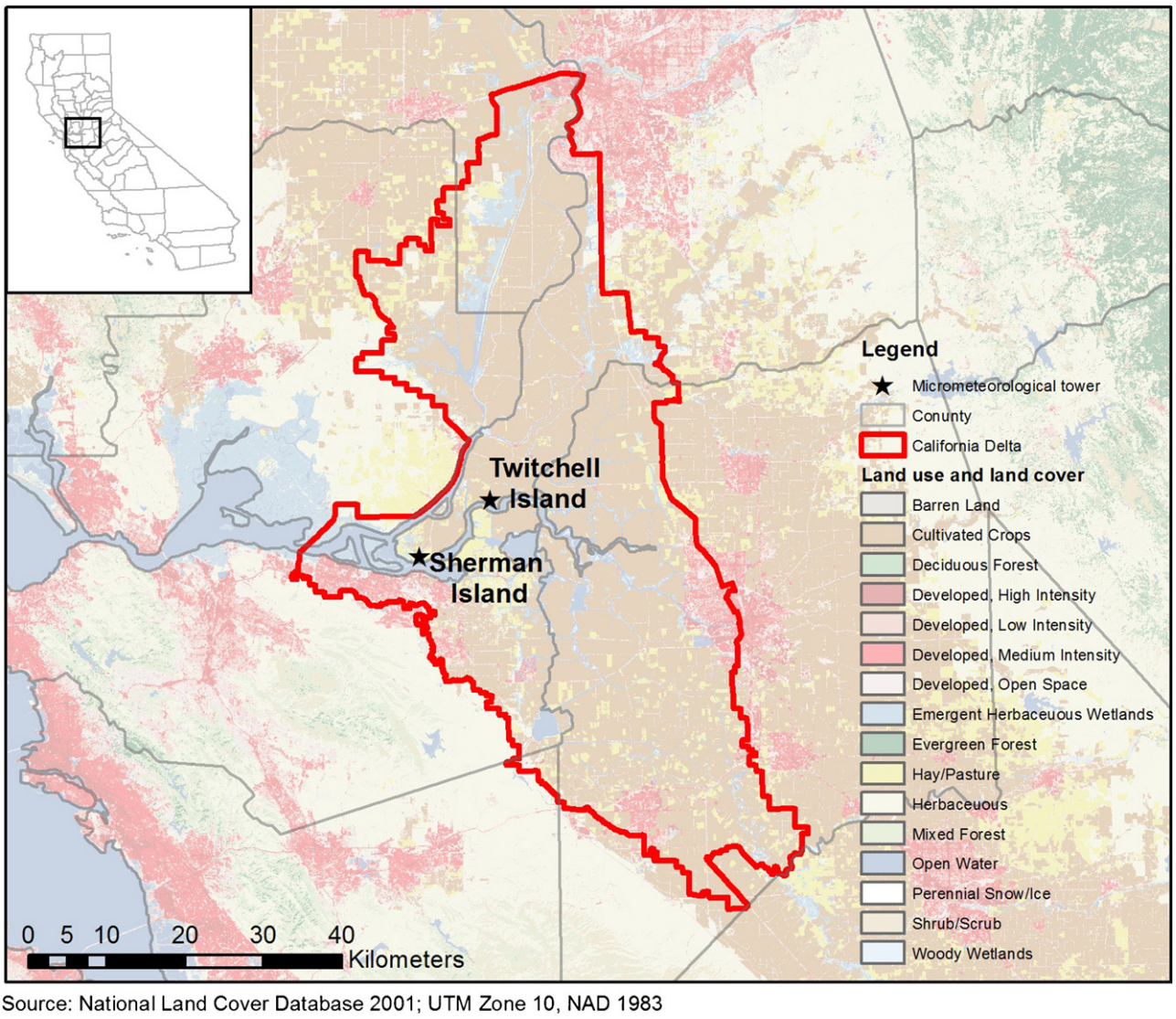

Fig. 1. Location of delta sites. The grazed degraded peatland and rice paddy are located in the Sacramento-San Joaquin Delta, inland of San Francisco Bay. Fluctuations in climate are nearly identical between sites, due to their close proximity (about 10 km). Pasture and cultivated crops are the dominant land-use types within the extent of the Delta.

change from drained to flooded ecosystems in the Delta on greenhouse gas, water, and energy exchange. Quantifying the magnitude and pattern of CO_2, CH_4, water, and energy fluxes from these two agricultural land-use types is essential for understanding the impacts of drained to flooded land-use conversion in the Delta. Through this framework, we evaluated the ability of the rice paddy to act as a land management opportunity for creating a sustainable Delta where farmers can maintain their livelihoods and transform Delta agriculture from a net carbon source to a carbon sink and stop subsidence. In addition to providing fundamental information about greenhouse gas fluxes in the Delta, this analysis also provides the data and metrics necessary to lay the groundwork for greenhouse gas accounting protocols and verification.

2. Methods

2.1. Study sites

Our two study sites are a drained and grazed degraded peatland on Sherman Island, CA (latitude: 38.0367°N; longitude: 121.7540°W; elevation: 12 m below sea level) and a rice paddy on Twitchell Island, CA (latitude: 38.1087°N, longitude: 121.6530°W; elevation: 14 m below sea level) (Fig. 1). Both sites are within the Sacramento-San Joaquin Delta approximately 100 km inland from the Pacific Ocean and they experience a Mediterranean climate, with hot, dry summers, and cool, wet winters. At the Anitoch climate station (10 km southwest of Sherman Island) the 50-year mean air temperature (1949–1999) is 15.1 °C and the mean annual precipitation is 335 mm. The water table at the grazed degraded peatland is regulated to 50–80 cm below the surface for the entire year. The water level at the rice paddy is maintained about 5–10 cm above the soil surface for most of the year, but it is drained twice annually: about 45 days before the start of the growing season for cultivation and planting, and for about 55 days at the end of the growing season for harvest.

The Sherman Island grazed degraded peatland site is covered by two invasive plants: mouse barley (*Hordeum murinum* L.) a C_3 grass that dominates the canopy December–April, and pepperweed (*Lepidium latifolium* L.) a perennial plant that dominates the canopy April–October. The effects of management decisions on plant canopy dynamics and carbon fluxes at the Sherman

Island grazed degraded peatland during 2007–2009 are discussed at length in Sonnentag et al. (2011a). The grazed degraded peatland (~0.9 km × ~0.4 km) is fenced and grazed year-round by approximately 100 cattle (about 1.1 animal acre^{-1}), which has been the land use maintained at the site for at least the past 20 years. During the summer months, the cattle aggregate in the far end of the field opposite the eddy covariance tower during the day, but the cattle pass by the tower frequently at evening and during winter months. Consequently, their presence can have a large impact on the methane and to a lesser extent, carbon dioxide, fluxes at the site (Detto et al., 2010; Baldocchi et al., in press).

The Twitchell Island rice paddy is a pilot project administered by the California Department of Water Resources (CADWR). The land was converted from traditional corn and alfalfa agriculture to rice (*Oryza sativa*) in 2009 to assess the feasibility of growing rice in the Delta. Before 1990, rice was not farmed in the Delta. Since then, development of new varietals that can withstand the cool nighttime growing season temperatures has made rice agriculture feasible in this region. Currently there are about 2000 ha of rice farmed in the Delta. The field where the eddy covariance tower is located is approximately 0.55 km × 0.7 km. The rice variety M104 (a cold-weather cultivar) was planted April 15 in 2009, and M206 (also a cold weather cultivar) was planted on April 16 in 2010. Rice was harvested October 22–25 in 2009 and October 28–29 in 2010. The field was fertilized with 30–0–20 ammonium sulfate fertilizer on May 27–28 in 2009, and on June 5–7 in 2010 at a rate of 68 kg acre^{-1}. In both 2009 and 2010 before planting, the drained rice fields were treated with herbicide (1.5 mg L^{-1} Bispyribac sodium and 2.5 mg L^{-1} Pendimethalin) and in 2010 the rice paddy was treated with additional herbicide the first week in June (3.65 g acre^{-1} Regiment, 324 g acre^{-1} Prowl, 32 g acre^{-1} SYL-TAC, 324 g acre^{-1} UN-32, and 4.1 g acre^{-1} Sandea) to remove a weed infestation that preceded rice growth. After harvest of the rice grains, the remaining plant residue was left on top of the soil in both 2009 and 2010, and the field was re-flooded for the winter months to provide habitat for migrating birds. During the flooded winter months, no plants grew within the field.

Each site is situated on degraded peat soil where the top-most layer is silt loam, overlaying a deep peat layer. At each site, we calculated soil bulk density gravimetrically by collecting samples within an aluminum collar (5 cm tall by 5 cm in diameter) at depths from 0 cm to 75 cm within the soil profile, drying, and then weighing each sample. After measurement for bulk density, we measured the percent carbon content and the carbon to nitrogen ratio of each sample by grinding the dried soil samples and analyzing them on a Shimadzu Elemental Analyzer. Soil parameters for both sites are outlined in Table 1. At both sites, the bulk density of the upper layer is higher and the carbon content is lower than the deeper soils layers, which generally contain more undegraded peat soil.

2.2. Micrometeorological measurements

Micrometeorological instruments were deployed at each site to accompany flux measurements made by the eddy covariance instruments. At each site, air temperature and relative humidity were measured with an aspirated and shielded thermistor and capacitance sensor (HMP45C; Vaisala, Vantaa, Finland). Precipitation was measured at both sites with a tipping rain bucket (TE525; Texas Electronics Inc., Dallas, TX, USA) and water table depth was measured with a pressure transducer (PDCR 1830; GE Druck, Billerica, MA, USA) located within a well at each site. Soil temperatures were measured at 2 cm, 4 cm, 8 cm, 16 cm, and 32 cm below the surface in three replicate profiles at each site with copper constantan thermocouples and the average of the three replicates at each depth was computed and used for analysis.

Net radiation (R_{net}) was measured at the grazed degraded peatland with a four-component net radiometer (CNR1; Kipp and Zonen, Delft, Netherlands) on a 2 m boom from the tower oriented toward the south. R_{net} at the rice paddy was measured with a two-component net radiometer (NRLite; Kipp and Zonen, Delft, Netherlands) on a 6 m boom oriented to the west. At both sites, incoming and outgoing photosynthetically active radiation was measured with quantum sensors as photosynthetic photon flux density (PAR-LITE; Kipp and Zonen, Delft, Netherlands). Ground heat flux was recorded by three replicate ground heat flux plates (HFP01; Huskeflux Thermal Sensors, Delft, Netherlands) buried 1 cm under the soil surface, and the average of the three replicates was used for analysis. All micrometeorological measurements were sampled every 5 s, and the 30 min mean values were stored on a CR10X datalogger (Campbell Scientific, Logan, UT, USA) at each site.

2.3. Eddy covariance measurements

The fluxes of CO_2, CH_4, H_2O, and energy were measured at each site with the eddy covariance (EC) method (Baldocchi et al., 1988). Briefly, the EC method calculates fluxes of a scalar of interest (for example, CO_2) by simultaneously measuring turbulent fluctuations in vertical wind and the scalar, and then computing the covariance between the two. We measured the covariance between turbulence and the scalar at 10 Hz intervals (every 0.1 s), and then computed fluxes as the average of the 10 Hz covariances over a thirty minute interval. This sampling rate and averaging interval allowed for a 5 Hz cut-off for the cospectra between turbulence and the scalar of interest, which was determined to be adequate for accurate eddy covariance measurements at these sites (Detto et al., 2011). The EC instrumentation used to calculate fluxes was mounted on a tower 3.15 m high at the grazed degraded peatland and on a tower 3.05 m high at the rice paddy. The prevailing wind direction at both sites is strongly from the west, as the sites are located within an inverted delta landform where winds from the Pacific Ocean are forced to travel inland through the Carquinez Strait, a narrow gap in the mountains of California's Coastal Range.

An almost identical set of EC instrumentation was deployed at each site. Each tower measured fluctuations in longitudinal, lateral, and horizontal wind directions (u, v, w; m s^{-1}), temperature (T_{sonic}), and the speed of sound with a sonic anemometer (Gill WindMaster Pro; Gill Instruments Ltd, Lymington, Hampshire, England). Fluctuations in CO_2 and H_2O density (ρ_{CO2}, ρ_{H2O}) were measured with an open-path infrared gas analyzer (LI-7500; LI-COR Biogeosciences, Lincoln NE, USA) and fluctuations in CH4 density (ρ_{CH4}) were measured with a closed-path, tunable diode laser fast methane sensor (FMA, Los Gatos Research, CA, USA). The sonic anemometer readings and ρ_{CO2}, ρ_{H2O}, and ρ_{CH4} densities were recorded at each site at 10 Hz intervals with a Campbell CR1000 datalogger (Campbell Scientific, Logan, UT, USA).

The FMA sensor requires an external pump to operate. At the grazed degraded peatland site, which had access to an AC power line, we deployed a scroll pump (BOC ESDP 30A, Edwards, Tewksbury, MA,USA) requiring 770 W of power and providing a flow rate of about 40 L min^{-1} at the FMA cell pressure (19 kPa). At the rice paddy, which requires a generator for electrical production, we deployed a diaphragm pump (N940.5APE-B, KNF Neuberger, Trenton, NJ, USA) requiring 240 W operating at 12 L min^{-1} at the FMA cell pressure in order to reduce power consumption. Extensive field testing was conducted to evaluate the performance of the FMA sensor at both sites (Detto et al., 2010).

Using standard eddy covariance techniques, we analyzed the 10 Hz data recorded for u, v, w, T_{sonic}, ρ_{CO2}, ρ_{H2O} and ρ_{CH4} to calculate half-hourly fluxes of sensible heat (H; W m^{-2}), CO_2 (NEE; μmol m^{-2} s^{-1}), H_2O (evaporation, latent energy (LE); mm m^{-2} s^{-1}, W m^{-2}) and CH_4 (nmol m^{-2} s^{-1}) after applying a series of

Table 1
Soil properties were measured at each field site. At both sites, the top layer has a higher bulk density and lower carbon content than the deeper layer, which contains partially undegraded peat soils. The soil parameters at the rice paddy were measured after one year of rice cultivation in the springtime while the field was drained, but before the field was planted or fertilized.

Site	Layer (cm below surface)	Soil type	Bulk density ($g\,cm^{-3}$)	Carbon content (%)	C:N
Grazed peatland	0–60	Degraded peat silt loam	1.08	7.5	13.9
Grazed peatland	60–75	Partially undegraded peat silt loam	0.95	15	15.6
Rice paddy	0–30	Tilled degraded peat silt loam	0.65	15	14.1
Rice paddy	30–45	Untilled partially undegraded peat silt loam	0.57	31	15.6

corrections using in-house software (Detto et al., 2010). In this software, the first data filter removed artificial spikes (values greater than six standard deviations of the mean within a one-minute window) and diagnostic instrument values that corresponded with bad readings, which were mostly correlated with rain or fog events. For each half-hour block of 10 Hz values that passed the first data filter, a coordinate rotation was applied to align the x-axis of the sonic anemometer to the mean wind direction by aligning the mean vertical and lateral velocities to zero. Within each half-hour block of fluxes, the effects of air density fluctuations were removed by the Webb–Pearman–Leuning correction (Webb et al., 1980; Detto and Katul, 2007). Fluctuations in T_{sonic} were calculated from fluctuations in the speed of sound after correction for crosswind and humidity effects (Schotanus et al., 1983; Kaimal and Gaynor, 1991). After applying the coordinate rotation and correcting for density fluctuations, we applied cospectral corrections following methods developed within Detto et al. (2011). The cospectral corrections are performed on the closed-path CH_4 fluxes to account for tube attenuation, the residence time in the cell, as well as sensor separation for CH_4, CO_2, and H_2O fluxes (Detto et al., 2011). After computing the fluxes, we filtered flux values with anomalously high and low friction velocity ($u_* > 1.2\,m\,s^{-1}$ and $|uw| < 0.02$) to constrain our analysis to periods where the air near the sensors was well-mixed, which removed 6% of possible 30-min rice fluxes in 2009–2010 and 7% in 2010–2011 and 9% of possible 30-min drained degraded pasture fluxes in 2009–2010 and 8% of drained degraded pasture fluxes in 2010–2011.

We assessed the random instrumental noise in each half-hour flux value using a bootstrapping technique. The bootstrap technique evaluated the covariance between w and the scalar of interest (T_{sonic}, ρ_{CO2}, ρ_{H2O} or ρ_{CH4}) on 100 bootstrapped samples taken with replacement from the actual distribution of 10 Hz values for w and the scalar for each half-hour. We then computed the standard deviation of calculated fluxes across the bootstrapped covariances. Resulting fluxes from wind directions outside of the footprint of the target land-use type (160–210° for both the grazed degraded peatland and the rice paddy) were filtered from the dataset and excluded from this analysis.

At the Sherman Island grazed degraded peatland, we conducted extra processing using higher-order statistics to filter out half-hour CO_2 and CH_4 fluxes when the cattle were in the footprint of the EC tower, as their presence dramatically alters the fluxes of CH_4, and to a lesser extent, CO_2 (Detto et al., 2010; Baldocchi et al., in press). Since cattle emit amounts of CH_4 that are orders of magnitude higher than the average soil flux at the drained grazed degraded peatland, their presence impacts the half-hour flux interval by creating a probability distribution function of 10 Hz ρ_{CH4} values that is markedly different from that of the background soil flux. The presence of cattle in the flux footprint creates a probability distribution of ρ_{CH4} and ρ_{CO2} that is skewed (3rd order statistical moment) and more outlier-prone (kurtosis, 4th order statistical moment) than the background ecosystem values. Furthermore, cattle leaving or entering the flux footprint is expected to create first and second-order unstationarity within the half-hour interval, which means that the mean ρ_{CH4} and its variance are not constant throughout the half-hour interval, but instead trends upward or downward with the movement of cattle. Since skewness of the normal distribution is zero, kurtosis of the normal is 3, and stationarity requires that the deviation from the long-term mean at a lagged point is zero, we can define periods when cows are likely within the field by the following criteria:

$$\left|\text{Skewness}\left(\overline{w'\rho'_{CH4}}\right)\right| > 3 \quad (1)$$

$$\text{Kurtosis}\left(\overline{w'\rho'_{CH4}}\right) > 10 \quad (2)$$

$$\left|1 - \frac{\overline{\left(w'\rho'_{CH4}\right)_{15\ min}}}{\left(w'\rho'_{CH4}\right)}\right| > 10 \quad (3)$$

where $(w'\rho'_{CH4})$ is the covariance between the 10 Hz values of w and ρ_{CH4}, and in the third criterion, $\overline{(w'\rho'_{CH4})_{15\,min}}$ is the mean covariance between w and ρ_{CH4} over a 15-min time interval and $(w'\rho'_{CH_4})$ is the mean covariance over the entire half-hour interval. We adopted the same filtering criteria to the ρ_{CO2} data to also remove periods heavily influenced by cattle at the drained peatland. We evaluated the accuracy of this statistical classification of fluxes at the grazed degraded peatland by comparing them to digital images of the tower footprint. A webcam (DCS-900; D-Link Corporation, Taipei, Taiwan) was installed on the EC tower, and a digital photograph was taken every half hour during daylight, at a lag that corresponded to the middle of the half hour interval used in the eddy covariance processing (Baldocchi et al., in press). In 2009–2010 at the degraded pasture 21% of possible 30-min fluxes were removed from the analysis by the cattle filter and 17% of possible fluxes were removed in the 2010–2011 year. Through this analysis it was determined that this statistical filter accurately eliminated fluxes heavily impacted by cattle metabolism.

2.4. Gap-filling, CO_2 partitioning, and integrating annual budgets

Using the half-hourly fluxes derived from eddy covariance, we computed the net annual budgets for evaporation, NEE, CH_4, and partitioned ecosystem photosynthesis (CO_2 uptake; P_{eco}) and ecosystem respiration (CO_2 release; R_{eco}) by gap-filling and subsequent integration. To gap-fill missing half-hourly fluxes, we used the artificial neural network (ANN) technique standardized within the international Fluxnet project, with meteorological variables driving the fitting (Papale and Valentini, 2003; Papale et al., 2006). While this technique has been used extensively for gap-filling H_2O and CO_2 fluxes, the ANN technique has not been applied to CH_4 fluxes, likely due to the limited studies of CH_4 fluxes using the eddy covariance technique (although Rinne et al. (2007) gap-filled an annual CH_4 budgets using meteorological drivers). For the purposes of this study, we only gap-filled the non-cow CH_4 flux for the grazed degraded peatland site, whereas at the rice paddy we gap-filled all data. At the drained degraded pasture gap-filled data comprised 38% of the 2009–2011 dataset and 32% of the 2010–2011 dataset, and at the rice paddy gap-filled data are 21% of the 2009–2010 dataset and 18% of the 2010–2011 dataset. These percentages represent data lost by all causes, including instrument malfunction and removal by data processing previously described, and the removal of cattle fluxes from the drained degraded pasture dataset explains

the larger percentage of gap-filled values at this site compared with the rice paddy.

Winds are strong even during the nighttime at both sites (Appendix A, Fig. A1), eliminating the need to account for uncertainties typically related to nighttime eddy covariance measurements due to nighttime atmospheric stratification and stability (Massman and Lee, 2002). To partition NEE into ecosystem photosynthesis (P_{eco}) and ecosystem respiration (R_{eco}), we applied the partitioning technique of Reichstein et al. (2005) to the ANN gap-filled NEE values. This method partitions NEE by extrapolating nighttime CO_2 flux as respiration using a short-term temperature response over 2 weeks using a temperature response function (Reichstein et al., 2005). By calculating the temperature response function on short timescales, this method accounts for seasonal changes in the temperature response due to confounding factors like substrate availability. This partitioning algorithm yielded results that followed an intuitive annual pattern for both sites, but we also investigated alternative partitioning algorithms to ensure that the Reichstein et al. (2005) method was the best choice for our data. We closely investigated the nighttime NEE data from both sites for patterns that would indicate a better partitioning of R_{eco} from the early evening maximum NEE method presented in van Gorsel et al. (2009). However, we were unable to justify the use of this method due to the relatively well-mixed nighttime conditions at the site and resulting lack of canopy storage of CO_2.

To compute annual sums, we integrated the gap-filled (and in the case of NEE, partitioned) fluxes from the ANN method over the course of each year within this study. We integrated the annual sums at the start of the rice growing season, from 25 April 2009 to 24 April 2010 as the first year, and 25 April 2010 to 24 April 2011 as the second year of the study. By using a bootstrapping procedure, we determined the amount of uncertainty in the ANN gap-filling procedure for the annual fluxes of each scalar (LE, NEE, P_{eco}, R_{eco}, and CH_4) (Hagen et al., 2006). We chose 1000 bootstrapped samples with replacement from the annual distribution of non-gap-filled half-hour fluxes of each scalar, and then gap-filled the bootstrapped samples. After gap-filling the bootstrapped samples we computed the integrated annual budget for each gap-filled bootstrapped annual dataset, and we calculated the 95% confidence interval from the distribution of the 1000 bootstrapped annual budgets. We calculated the annual potential evaporation (LE_{pot}) at each site based on the Penman equation (Penman, 1948) as in Shuttleworth (2007) from our measurements of R_{net}, wind speed, vapor pressure deficit, and air temperature.

2.5. Vegetation sampling methods

Plant area index (PAI) was measured every 1–2 weeks at the grazed degraded peatland and the rice paddy during the growing season by both destructive (direct) and nondestructive (indirect) measurements. We call our measurements PAI rather than leaf area index because at both sites we did not separate leaves from other plant matter. We measured PAI every 2–4 weeks over the winter at the grazed degraded peatland by direct measurement only, due to the short stature of winter grasses at the site. Destructive PAI measurements were conducted at each site by clipping all aboveground biomass within five randomly sampled 400 cm^2 plots. We then measured the area of each sample using an optical area scanner (LI-3100 area analyzer; LI-COR Biogeosciences, Lincoln NE, USA). Using these areas, we calculated PAI as area of all standing biomass within each plot divided by the area of the plot (400 cm^2). Indirect PAI measurements were made with the LAI-2000 Plant Canopy Analyzer (LI-COR) during months when the height of vegetation was greater than 0.5 m. PAI measurements with the LAI-2000 were made every 10 m along a 100 m transect extending west into the predominant wind direction at the rice paddy, and every 10 m along a 200 m transect extending in the east-west direction at the grazed degraded peatland site according to the protocol in Sonnentag et al. (2011a).

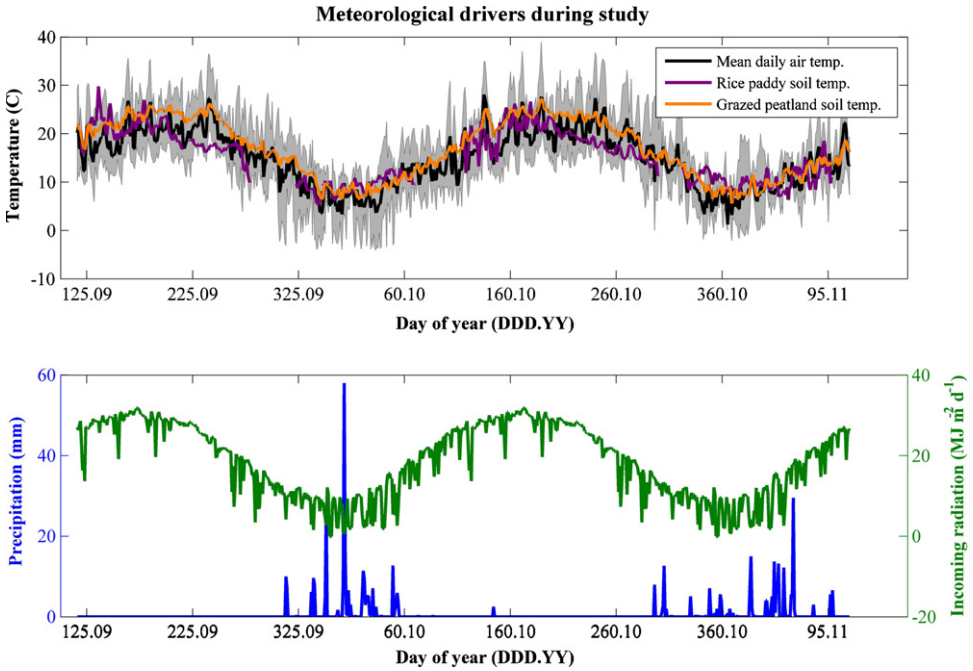

Fig. 2. Meteorological drivers during study. The top panel shows the mean daily air temperature and soil temperatures at 2 cm depth for each site, where the gray shaded area bounds the minimum and maximum daily air temperature. Air temperature is only plotted for the grazed degraded peatland since values for the rice paddy were nearly identical. The flooded status of the rice paddy during the summer months creates a lower average soil temperature than the drained and grazed degraded peatland. The bottom panel demonstrates the typical pattern of a Mediterranean climate at these sites, with high incoming solar radiation and very little rainfall during the summer months, and wet, cool winters.

3. Results

3.1. Micrometeorology and the energy balance

Trends in meteorological variables at the two sites follow a strong seasonal cycle as a result of the distinct Mediterranean climate within the Delta (Fig. 2). Mean air temperatures for May 2009–April 2010 were 15.0 °C at the grazed degraded peatland and 14.2 °C at the rice paddy, and for May 2010–April 2011 mean air temperatures were 14.8 °C at the grazed degraded peatland and 13.9 °C at the rice paddy, not far from the 50-year (1949–1999) mean of 15.1 °C from the Antioch Climate Station 10 km from the grazed degraded peatland site (Table 2). Total precipitation was 438 mm for May 09–April 10 and 404 mm for May 10–April 11, slightly greater than the 50-year mean of 335 mm, and total incoming radiation was 6878 MJ m^{-2} yr^{-1} from May 2009 to April 2010 and 6934 MJ m^{-2} yr^{-1} from May 2010 to April 2011. When the rice canopy is closed (PAI > 2) and the rice paddy is flooded (15 July–1 October), the soil is shaded by the dense rice canopy, soil temperatures ($T_{s,grow}$) are on average 3.5–4.5 °C lower than the grazed degraded peatland soils (Table 2). Such a decrease in soil temperature may help to diminish heterotrophic respiration during the rice growing season, and thus help diminish peat oxidation, as Deverel and Rojstaczer (1996) showed significant correlations of log of carbon dioxides fluxes with soil temperature for chamber measurements on three Delta islands. Our results indicate that generally, there are only very small differences between the two sites with respect to basic meteorological drivers of ecosystem form and function. However, these two land-use types fundamentally differ in the way that they utilize the available incoming energy by mechanisms that correspond to differences in their vegetation cover and water management.

While the annual net radiation (R_{net}) is similar between the two sites (Table 2), differences in the water management (drained versus flooded) as well as the canopy cover (Fig. 3) drive differences in the way the energy balance is distributed between sensible and latent heat exchange. As is evident in Fig. 3, the PAI at the rice paddy demonstrates a short pattern of vegetative growth with low interannual variability due to the crop cycle, whereas the PAI at the grazed degraded peatland is much more variable, both between and within sampling dates, due to the complex phenology of pepperweed (Sonnentag et al., 2011b). While the rice paddy has a short but intense period of vegetation for a small part of the year, the grazed degraded peatland demonstrates vegetative growth throughout the year, which changes meteorological variables connected to the canopy structure. For the two years in this study, the grazed degraded peatland is relatively balanced between sensible and latent heat exchange on an annual basis, while the energy balance of the rice paddy is dominated by high rates of latent heat exchange, mostly during the summer growing season (Table 2; Fig. 4). At the rice paddy, actual evaporation was 102% of potential evaporation from May 2009 to April 2010 and 91% of potential evaporation from May 2010 to April 2011, while at the grazed degraded peatland, actual evaporation was 52% of potential evaporation in the first year, and 63% of potential evaporation in the second year. At the rice paddy, inundation and the maintenance of a dense plant canopy during the warmest time period in the summer buffers sensible heat exchange, increases latent heat exchange, and decreases mean soil temperature when compared with the grazed degraded peatland. The energy balance is less variable throughout the year at the grazed degraded peatland, due to the more continuous plant canopy when compared with distinct growing season during half the year at the rice paddy. The daily energy balance closure of both sites, defined as the slope between the sum of daily H, LE, and G and daily measured R_{net} was 0.85 at the grazed degraded peatland. At the rice paddy, we also accounted for heat storage in the water column as the daily change in water depth multiplied by the specific heat of water, and daily energy balance closure was 0.94 (Appendix A, Fig. A2). Hourly energy balance closure at the grazed degraded peatland 76% and at the rice paddy was 65%, within the bounds typically measured at eddy covariance towers across the FLUXNET network of sites (Wilson et al., 2002). The lower energy balance closure at the rice paddy is likely due to the rough approximation of heat storage in the water column in this study, as the change in water temperature was only measured at a single depth in the water column.

3.2. H_2O fluxes and annual budgets

Both sites had similar seasonal cycles of evaporation, as they evaporated the most water during the summer when high incoming solar radiation drives soil evaporation at the rice paddy and plant growth and maintenance drive transpiration at both sites (Fig. 4). The rice paddy evaporated up to 10 mm d^{-1} during the summer growing season, but rates dropped to below 2 mm d^{-1} during the winter, even though the surface is covered by exposed water over winter (Fig. 4). The grazed degraded peatland had more moderate rates of evaporation throughout the course of the year, evaporating 4–7 mm d^{-1} during the spring and early summer, and about 2 mm d^{-1} during the winter (Fig. 4). The grazed degraded peatland had notably higher evaporation than the rice paddy in winter, when grasses at the grazed degraded peatland transpired water, compared with the fallow canopy at the rice paddy.

Despite this slightly higher wintertime rate, the rice paddy evaporated a much larger amount of water on an annual basis when compared to the degraded peatland. The rice paddy evaporated 1207 mm water in 2009–2010 and 1111 mm water in 2010–2011, while the grazed degraded peatland evaporated 614 mm and 757 mm

Table 2
This table outlines the mean air temperatures (T_{air}), soil temperatures at 2 cm depth (T_s), and growing season soil temperatures at 2 cm depth ($T_{s,grow}$) for each site and year in this study. The radiation budgets for each site in each year are also presented for total incoming radiation (R_g), net radiation (R_{net}), sensible heat exchange (H), and latent heat exchange (LE), with the bootstrapped 95% confidence intervals for the gap-filling procedure in the parentheses. While both sites receive the same amount of incoming and net radiation due to their spatial proximity, the way that the two land-use types partition the budget of R_{net} is markedly different. While the grazed degraded peatland is more balanced between H and LE, most of the energy exchanged at the rice paddy is due to LE.

Site	Year	T_{air} (°C)	T_s (°C)	$T_{s,grow}$ (°C)	R_g (MJ m^{-2} yr^{-1})	R_{net} (MJ m^{-2} yr^{-1})	H (MJ m^{-2} yr^{-1})	LE (MJ m^{-2} yr^{-1})	LE_{pot} (MJ m^{-2} yr^{-1})[a]
Grazed degraded peatland	2009–2010	15.0	16.5	22.8	6878	2998	764 (734–794)	1507 (1477–1538)	2886 (α^b = 0.71)
	2010–2011	14.8	16.3	21.7	6934	3027	589 (560–624)	1858 (1819–1896)	2950 (α = 0.88)
Rice paddy	2009–2010	14.2	15.6	18.2	6878	3354	138 (105–180)	2960 (2888–3024)	2916 (α = 1.24)
	2010–2011	13.9	15.3	18.4	6934	2977	211 (185–240)	2724 (2663–2791)	3021 (α = 1.25)

[a] Potential evaporation (LE_{pot}) is calculated by the Penman equation after (Shuttleworth, 2007).
[b] $\alpha = LE/LE_{eq}$ where LE_{eq} is equilibrium evaporation, and is equal to $(R_{net} - G)(s/(s+\gamma))$.

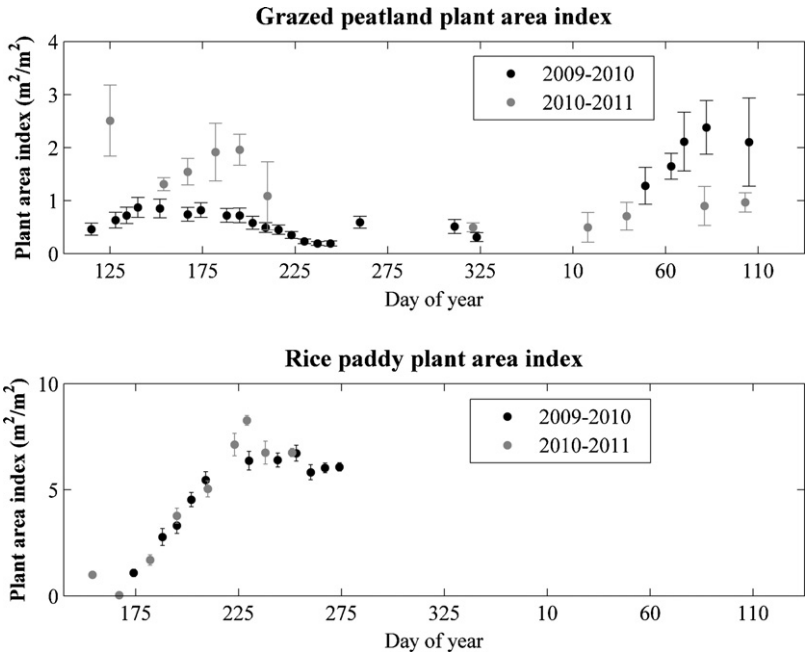

Fig. 3. Plant area index. The plant area index was sampled at each site throughout the study period. The error bars represent standard error in the measurements with at least five samples represented by each point, and the error bars on rice paddy data are present, but some bars are too small to visualize due to low variation within sampling dates. The pattern of plant area reaches its maximum during the summer months at the rice paddy, and during the early spring at the grazed degraded peatland. While the pattern of plant growth is predictable and demonstrates very little interannual variation at the rice paddy, the pattern is much more heterogenous between years and within individual sampling dates at the grazed degraded peatland due to the complex vegetation dynamics of the pepperweed plant (Sonnentag et al., 2011b).

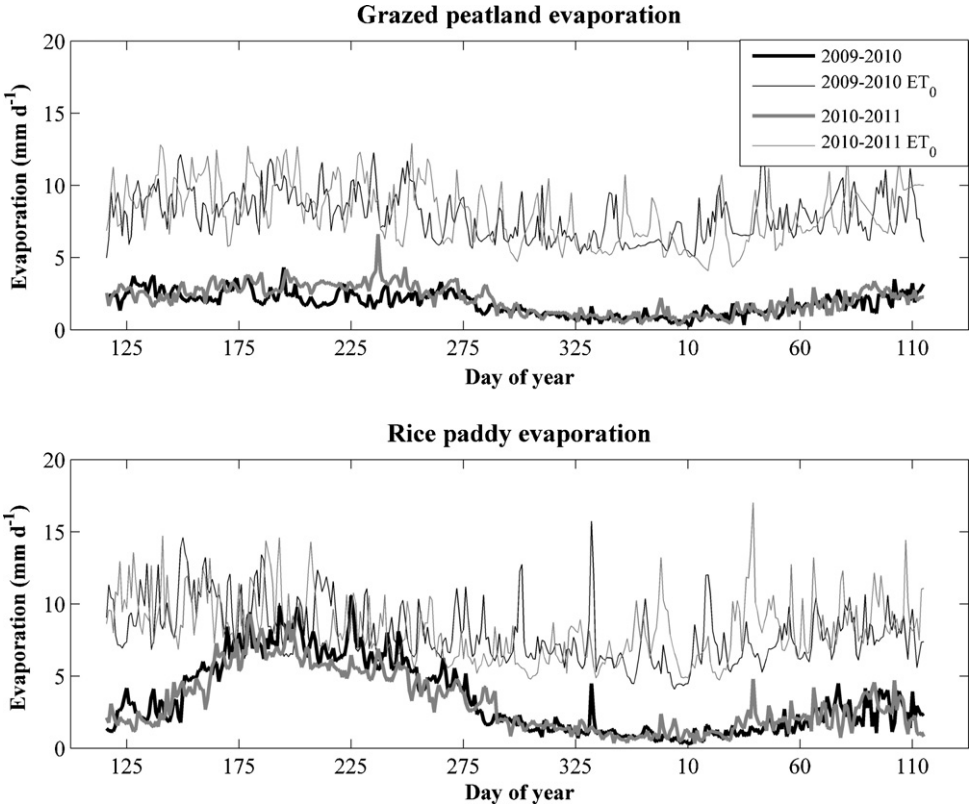

Fig. 4. Evaporation. The evaporation fluxes (thick lines) at the two sites follow the same seasonal cycle, with high rates of evaporation during the summer months, and low evaporation during the winter. The potential evaporation, calculated by the Penman equation (thin lines) was significantly higher than the grazed peatland evaporation for the whole year, but matched the rice paddy evaporation during the growing season. The grazed degraded peatland has slightly higher winter evaporation than the rice paddy due to transpiration by the grass canopy, whereas there are no plants at the rice paddy over winter to evaporate water. There is also more interannual variability in the H_2O fluxes at the grazed degraded peatland than at the rice paddy due to larger changes between years in the plant canopy at the grazed degraded peatland.

in those respective years. The annual budget of evaporation at the rice paddy was 94% higher than the grazed degraded peatland for the 2009–2010 budget and 47% higher than the grazed degraded peatland for the 2010–2011 budget (annual sums in Table 3). The evaporation budget at the grazed degraded peatland had more interannual variability than that of the rice paddy due to higher variability in the canopy leaf area index (Fig. 3), creating higher variability in the annual budgets of evaporation for the two years in this study. Whereas the maximum PAI was about 1 during the 2009 growing season, PAI reached up to 2.5 during the 2010 growing season, evaporating more water than in 2009.

3.3. CO_2 fluxes and annual budgets

The overall pattern in NEE at both sites followed a similar seasonal cycle (Fig. 5), as most photosynthesis occurred in spring and summer, corresponding to the period with high incoming solar radiation. The highest rates of CO_2 uptake at the grazed degraded peatland, about -4 g-C m^{-2} d^{-1}, occurred in late spring and corresponded with pepperweed growth. Even though there is a total absence of rain at the grazed degraded peatland during the late spring and summer and surface soil moisture is very low (about 7–15% volumetric water content), plant growth is nonetheless possible because pepperweed can tap the shallow water table, which is maintained by managers at about 50 cm below the grazed degraded peatland surface year-round. The highest rates of CO_2 release at the grazed degraded peatland corresponded to the period of the return of autumn rainfall, and reached about 8 g-C m^{-2} d^{-1} of net CO_2 emissions to the atmosphere during this time. The highest rate of NEE uptake at the rice paddy corresponded with high rice photosynthesis during the middle of the growing season, and reached about -12 g-C m^{-2} d^{-1}. The highest period of net emission of CO_2 to the atmosphere at the rice paddy corresponded with drainage events, and averaged about 6 g-C m^{-2} d^{-1}.

High rates of photosynthesis but even higher rates of respiration at the grazed degraded peatland made it a net source of CO_2 to the atmosphere in both years of this study. The grazed degraded peatland released 299 g-C m^{-2} as CO_2 in 2009–2010, and 174 g-C m^{-2} in 2010–2011. Annual budgets in this study were a larger net source of CO_2 than in 2008–2009 due to the regrowth of pepperweed following a mowing event in early summer 2008 (a common land management practice in Delta pasture) (Sonnentag et al., 2011a). Differences in the annual NEE budget at the grazed degraded peatland between years (Fig. 5) were primarily caused by an increase in plant growth during the 2010 growing season (Fig. 3), as pepperweed continued to recover after the 2008 mowing event.

While the grazed degraded peatland and rice paddy captured similar amounts of CO_2 through ecosystem photosynthesis in both of the studied years, the CO_2 lost through R_{eco} is smaller at the rice paddy when compared with the grazed degraded peatland (Fig. 6). The rice paddy acted as a net sink for CO_2 in both years, capturing 84 g-C m^{-2} as CO_2 from the atmosphere in 2009–2010 and 283 g-C m^{-2} in 2010–2011 (sums in Table 3). Differences in the net budget of CO_2 at the rice paddy between years were caused by higher rates of P_{eco} in 2010–2011 than 2009–2010, resulting in higher CO_2 uptake. Although the rice growing season extends for only half the year, ecosystem photosynthesis captures about the same amount of CO_2 as the year-round grazed degraded peatland vegetation, and P_{eco} at the two sites only differs by about 50–75 g-C m^{-2} yr^{-1} (Table 3).

Differences in the processes that control R_{eco} at each site caused variation in the seasonal pattern of R_{eco} at the grazed peatland and rice paddy (Fig. 6). Upon the return of the autumn rains to the Delta, rates of R_{eco} at the grazed degraded peatland increased as moisture at the surface renews microbial activity, and R_{eco} increased from its summertime rate of about 5 g-C m^{-2} d^{-1} to 8 g-C m^{-2} d^{-1}. At the rice paddy, the winter season is a period of low rates of R_{eco}, since decomposition and respiration occur much more slowly in the flooded and unvegetated conditions that are maintained for migrating birds. R_{eco} at the rice paddy is nearly always lower than 5 g-C m^{-2} d^{-1}, with the exception of drainage events that create large pulses of CO_2 to the atmosphere. Thus, while the presence of additional water during the winter months through precipitation stimulates R_{eco} at the grazed degraded peatland, total inundation at the rice paddy inhibits R_{eco}.

3.4. CH_4 fluxes and annual carbon budgets

Large differences exist in both the magnitude and seasonal pattern of CH_4 fluxes at the grazed degraded peatland and rice paddy (Fig. 7). The grazed degraded peatland CH_4 fluxes in 2009–2010 and 2010–2011 had a very low and stable rate of CH_4 emission ranging from 1 mg-C m^{-2} d^{-1} to 10 mg-C m^{-2} d^{-1}, which increased slightly during the wetter winter months when compared with the summer when the soil surface is very dry. This pattern of degraded peatland soil CH_4 flux matches well with previous studies at the site, which concluded that the background soil flux is low, but occasionally dominated by high fluxes from wet drainage ditches, which are more frequently inundated during winter (Teh et al., 2011). The gap-filled CH_4 budget accounting for background ecosystem flux released 3.32 g-C m^2 as CH_4 to the atmosphere during 2009–2010, but we did not collect enough CH_4 flux data in 2010–2011 to reliably compute the annual sum.

The CH_4 fluxes in the first year of rice paddy measurements (2009–2010) were low at about 10 mg-C m^{-2} d^{-1}, and did not follow a strong pattern (Fig. 7). However, the CH_4 fluxes during the 2010 growing season followed a seasonal pattern as they paralleled P_{eco} of the rice (Fig. 6) and peaked during drainage of the field in late

Table 3
The annual sums of the H_2O, partitioned CO_2, and CH_4 fluxes (with the bootstrapped 95% confidence intervals for the gap-filling procedures in parentheses) are presented for each site during each year of the study. Positive values indicate sources to the atmosphere, and negative values are sinks from the atmosphere. At the grazed degraded peatland, the FMA CH_4 sensor did not run for the second half of the 2010–2011 time periods, so we considered it imprudent to calculate the grazed degraded peatland CH_4 budget for this year. In both years, the grazed degraded peatland acted as a net source of carbon to the atmosphere, and the rice paddy acted as a net sink for carbon, although CH_4 fluxes at the rice paddy in 2010–2011 increased dramatically compared with the first year of this study. The grazed degraded peatland evaporated water than the rice paddy in both years, and generally demonstrated more interannual variability for H_2O and CO_2 exchange due to higher variation in PAI between years.

Site	Year	H_2O (mm y^{-1})	NEE (g-C m^{-2} y^{-1})	R_{eco} (g-C m^{-2} y^{-1})	P_{eco} (g-C m^{-2} y^{-1})	CH_4 (g-C m^{-2} y^{-1})	Total CO_2-equivalent (g-C m^{-2} yr^{-1})
Grazed degraded peatland	2009–2010	614 (602–627)	299 (222–373)	1493 (1418–1582)	−1182 (−1231–1137)	3.3 (2.8–3.9)	382 (293–471)
	2010–2011	757 (741–772)	174 (113–233)	1765 (1691–1850)	−1557 (−1604–1506)	N/A	N/A
Rice paddy	2009–2010	1207 (1178–1234)	−84 (−118–43)	1176 (1145–1209)	−1258 (−1290–1227)	2.5 (2.1–2.9)	−22 (−63–29)
	2010–2011	1111 (1086–1138)	−283 (−344–226)	1350 (1297–1395)	−1577 (−1630–1525)	6.6 (6.1–7.0)	−119 (−192–52)

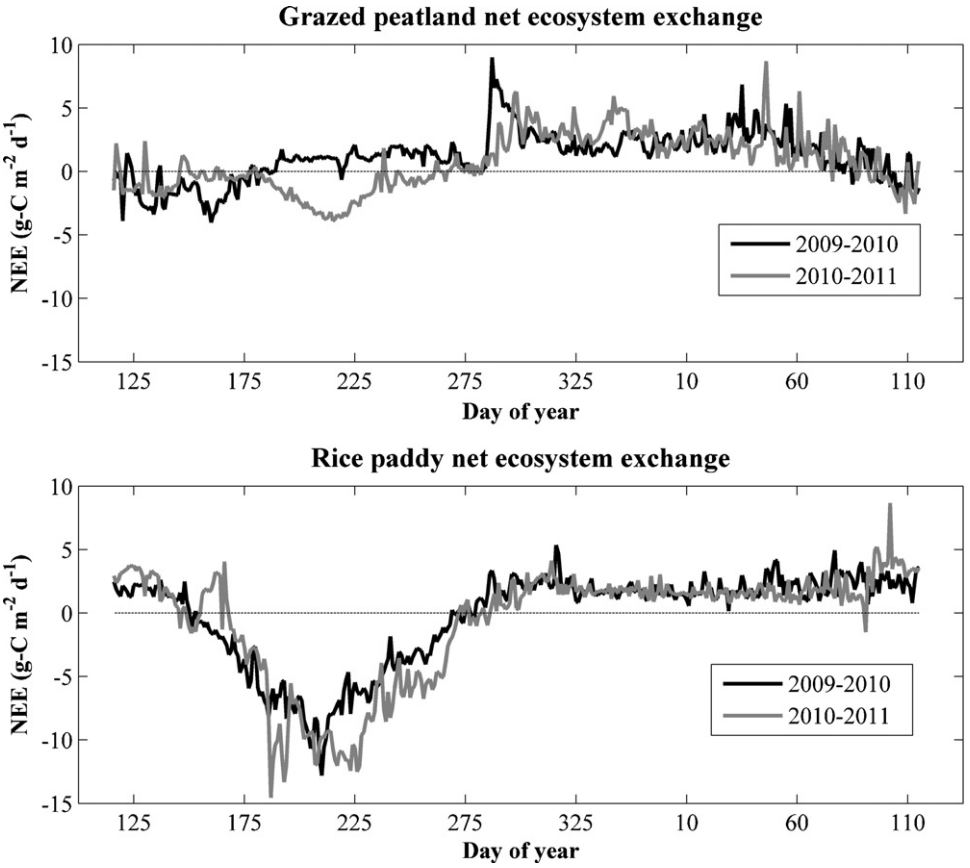

Fig. 5. Net ecosystem exchange. The net ecosystem exchange at each site follows a seasonal pattern with the growing season with highest carbon uptake in the spring and summer and highest carbon efflux during winter. Error bounds derived from bootstrapping the half-hourly EC fluxes are not included in this figure since they are too small to visualize, as the 95% bounds of bootstrapped values varied only 5.1% from the measured CO_2 fluxes at the grazed degraded peatland and 4.3% of measured CO_2 fluxes at the rice paddy.

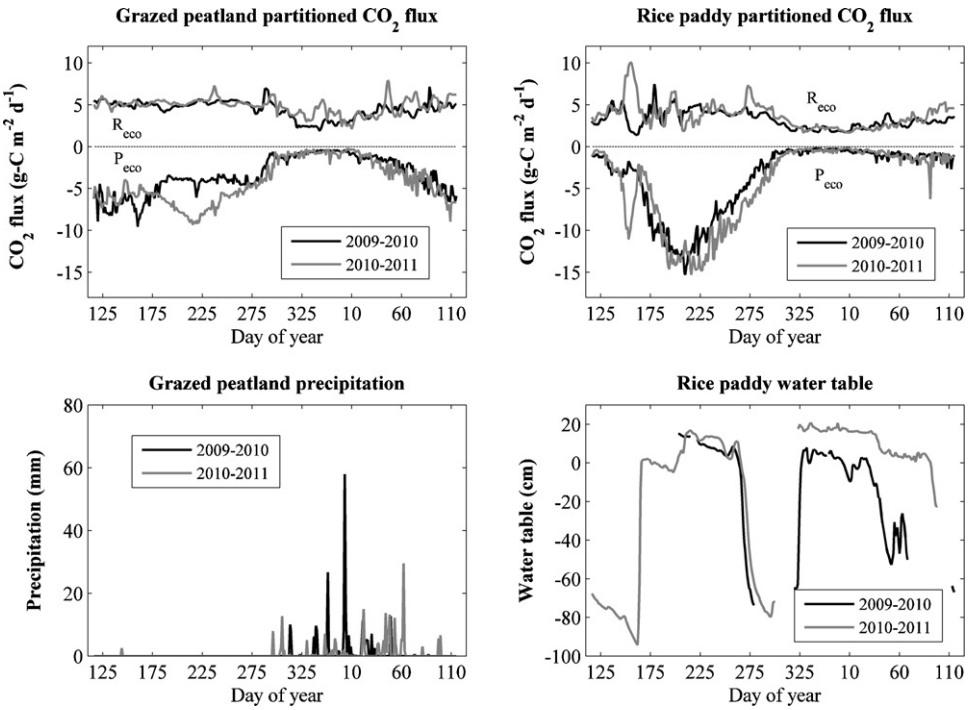

Fig. 6. Partitioned CO_2 fluxes. The partitioned CO_2 fluxes for the grazed degraded peatland and the rice paddy site follow the same pattern of CO_2 uptake during the summer growing season. There is large interannual variability in the GEP at the grazed degraded peatland site, whereas the rice paddy shows less variation between the two years. Whereas peaks in respiration at the grazed degraded peatland are primarily governed by precipitation pulses, respiration at the rice paddy is closely tied to changes in the water table. While the addition of water by precipitation at the grazed degraded peatland has the effect of stimulating ecosystem respiration, the addition of water by flooding at the grazed degraded peatland suppresses ecosystem respiration.

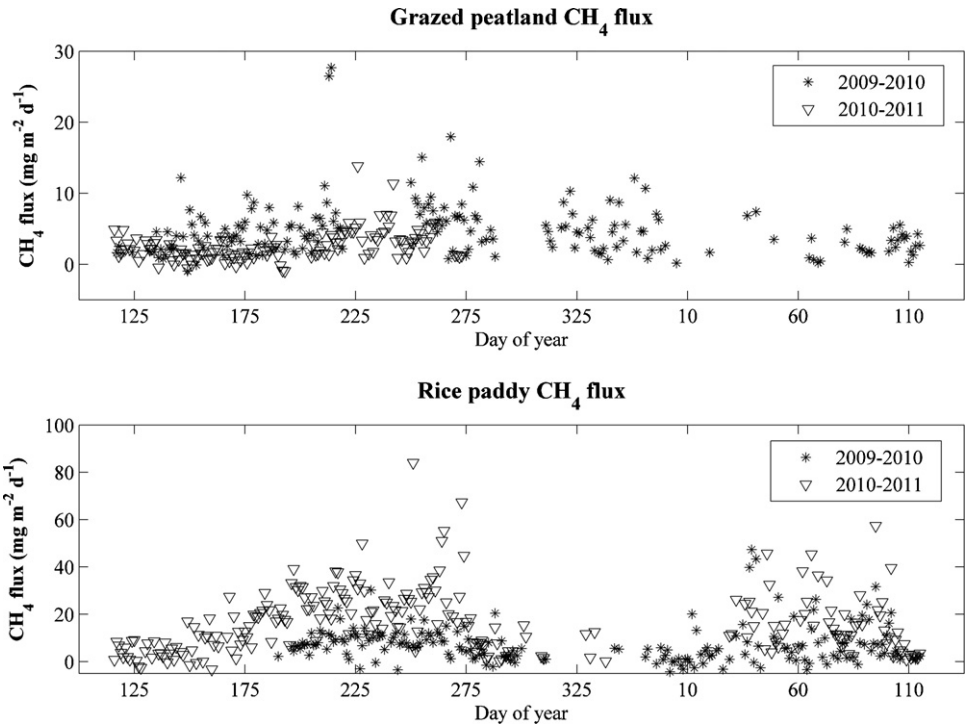

Fig. 7. Methane. Daily integrated CH_4 flux at each site for days when there was a measured flux for at least half of the possible 48 half-hour intervals. Values are missing for many days due to instrument malfunction and/or power supply issues at the sites, particularly during the winter months. The CH_4 sensor was removed from the grazed peatland on DOY 276 in 2010, so no values appear after this date. At the grazed degraded peatland, there are many missing values due to the filtering of fluxes when cows were present in the tower footprint. Soil fluxes at the grazed degraded peatland are generally low, although slightly higher in the wetter winter months. Although CH_4 flux was generally low at the rice paddy during the 2009 growing season, the CH_4 flux in the 2010 growing season was much larger, and followed a pattern that matched that of gross primary productivity.

September, a pattern more typical of other rice paddy studies. While the CH_4 flux was near zero in the beginning of the 2010 growing season, by August the rice paddy was emitting about 40 mg-C m^{-2} d^{-1} as CH_4. In the 2009–2010 annual budget the rice paddy released 2.5 g-C m^{-2} as CH_4 to the atmosphere and in 2010–2011 the rice paddy released 6.6 g-C m^{-2}.

Using the climate warming factor for CH_4 as 25 times that of CO_2 on a 100-year horizon (Forster et al., 2007), the CH_4 emissions from the grazed degraded peatland in 2009–2010 were 83 g-C m^{-2} CO_2 equivalent. The same calculation for the rice paddy CH_4 emissions yields 63 g-C m^{-2} CO_2 equivalent in 2009–2010 and 165 g-C m^{-2} CO_2 equivalent in 2010–2011. While the grazed degraded peatland emitted about 25% more CH_4 than the rice paddy in the first year, assuming that the grazed degraded peatland would have emitted the same amount in 2010–2011, the rice paddy would have emitted about 50% more CH_4 than the grazed degraded peatland in the second year of this study. We also point out the relatively high uncertainty regarding the extrapolation of the annual CH_4 budget from these data due to the large amount of data missing due to power failures, instrument malfunction, and filtering due to cow presence at the grazed degraded peatland.

Using a CO_2-equivalent warming factor conversion for the annual CH_4 budget calculations of 25, we determined that the CO_2-equivalent carbon budget at both sites still follows the same trend that the annual NEE budgets indicated: the grazed degraded peatland emitted 382 g-C m^{-2} CO_2 equivalents in 2009–2010, and the rice paddy captured 22 g-C m^{-2} in 2009–2010 and 119 g-C m^{-2} in 2010–2011, even after accounting for the higher-impact emissions of CH_4 (Table 3). We caution that these numbers represent emissions only after two years of land-use conversion, which is a relatively small time scale for ecological changes, and the rice paddy might continue to emit more CH_4 each year as data collection at these sites continues into the future.

4. Discussion

4.1. Water vapor

In the first year of the study, the rice paddy evaporated about 94% more water than the grazed degraded peatland site, and in the second year evaporation at the rice paddy exceeded grazed degraded peatland evaporation by about 47% (Fig. 4; Table 3). This pattern matches our expectations, since the higher water table at the rice paddy is more directly exposed to the atmosphere. In addition to these fundamental differences in the annual budget due to differences in water table management, additional variability in the seasonal evaporation from each site can be explained by the differences in vegetation cover. The grazed degraded peatland has year-round vegetation cover, as pepperweed grows during the summer and grass during the winter, continually transpiring water from the soil to the atmosphere. At the rice paddy, although the water surface is directly exposed to the atmosphere during winter, there is much lower evaporation due to the very low amount of incoming radiation at this point in the year due to both the low solar angle and winter rain and fog (Fig. 2). Thus, transpiration at the grazed degraded peatland due to the growth and maintenance requirements of the winter grasses outpaces the small amount of evaporation from the exposed water surface at the rice paddy.

A week-long study on the energy balance at a Japanese rice paddy found that rates of evaporation were near potential evaporation, although at rates from 4.2 mm d^{-1} to 5.8 mm d^{-1} the magnitude of evaporation was lower than in our study, likely due to the lower vapor pressure deficit when compared with our site (Harazono et al., 1998). Earlier measurements throughout the growing season at another Japanese rice paddy found similar results, with daily evaporation rates near 5 mm d^{-1}, again lower than the rates in our study likely due to the high incoming solar radiation at our site (Uchijima, 1976). Our study reaches similar conclusions as those from an early lysimeter study at a rice paddy near Davis, CA (about 55 km north of Twitchell Island, but climatically warmer and less windy than the Delta), which demonstrated that rice agriculture at this site on average evaporated about 1100 mm yr^{-1}, but that this evaporation budget is only 3.5% higher during the growing season than fescue, a common pasture crop of the area (Lourence and Pruitt, 1971). Thus, while it seems like the differences in evaporation between the rice paddy and grazed degraded peatland are large, evaporative sums might be closer

between the rice paddy and other traditional irrigated crops grown on drained soil in the Delta. In a year-long study of evaporation from five irrigated grass pastures at locations throughout California's Central Valley, experimenters found rates of evaporation that ranged from 1035 mm yr^{-1} to 1315 mm yr^{-1} (Pruitt et al., 1972), which is very similar to the evaporation rates of rice measured in this study (Table 3). Corn, the dominant Delta crop, evaporates about 580–690 mm of water just during the growing season (May–September) (Hoffman et al., 1983).

The evaporation rates of a restored marsh on Twitchell Island measured from 2002 to 2004 also fall within the same range as the measurements in this study; mean evaporation was about 6 mm d^{-1} during the course of the year, and the annual budget ranged from 1480 mm yr^{-1} to 1530 mm yr^{-1} (Drexler et al., 2008). Evaporation fluxes at a southern California marsh were much lower, with peak evaporation rates near 5 mm d^{-1} in midsummer (Goulden et al., 2007). Rates of evaporation from the rice paddy were similar to those from a riparian cottonwood forest about 50 km east of the Delta, which evaporated 1095 mm yr^{-1} (Kochendorfer et al., 2011). The results from our study can also be compared with evaporation rates from 2 long-term AmeriFlux sites in an oak savanna and grassland located about 60 km east of the Delta sites, which are climatically similar to the Delta, but are located on mineral soils with a much deeper water table. Evaporation of the grassland over six years averaged 319 mm yr^{-1} (Ryu et al., 2008), and that of the oak savanna ranged from 320 mm yr^{-1} to 469 mm yr^{-1} over seven years Baldocchi et al., 2010. This demonstrates the strong control that water availability plays in determining rates of evaporation in Mediterranean climates. At the rice paddy, the water surface is exposed to the atmosphere, driving much higher rates of evaporation, while at the grazed peatland the ability of the pepperweed plant to tap shallow water table drives higher rates of transpiration.

Differences in the evaporative balance between the grazed degraded peatland and rice paddy translate to differences in the latent heat exchange budgets due to the timing of evaporation during the year at the two sites. Because the rice paddy loses nearly its entire annual evaporation budget during the hot summer months and latent heat exchange is a function of air temperature and vapor pressure deficit, the latent heat budget of the rice paddy is much higher than that of the grazed degraded peatland on an annual basis (Table 2). Thus, although the two sites have similar levels of net radiation, the energy budget at the rice paddy is heavily weighted toward latent heat exchange, which might create a net cooling effect on the local climate at the rice paddy when compared with the grazed degraded peatland. Although our study included only two years of data, we can reasonably assume that the water use at the rice paddy will not demonstrate drastic interannual variability between growing seasons due to the regularity of the rice canopy structure between years (Fig. 3), and thus the rice paddy can be expected to evaporate a similar amount of water into the atmosphere in future years. There may be more interannual variability at the grazed degraded peatland that parallels changes in the canopy structure at the site (Fig. 3).

The relatively high rates of evaporation from the rice paddy within our study might be considered a negative consequence for the water budget in California, but high evaporation rates at the rice paddy also yield some benefits. On Twitchell Island, much of the water supply for the rice is pumped from island drainage ditches and recirculated rice drain water, which reduces the need for pumping of drainage water from the island. Conversion of entire islands to rice will eliminate the need for removing shallow groundwater to maintain a drained root zone and thus provide greater drainage control and reuse opportunities which will likely reduce pumping costs. Since the Delta islands where the sites are located are below sea level, land managers are required to expend large amounts of fossil fuels constantly pumping water out of the islands to prevent flooding. Pumping water throughout California is one of the highest consumers of electricity production, and thus reducing the amount of required pumping by increasing evaporation might help to alleviate some of the fossil fuels needed to regulate water supply on the islands. Conversion of Delta islands to rice production will also reduce the hydraulic forces on levees and seepage through levees. Raising the average groundwater table by about 1 meter will reduce the hydraulic gradients onto islands and thus reduce seepage, further reducing drainage pumping costs and fossil fuel consumption. Using groundwater flow modeling, Deverel et al. (2007) estimated that seepage will be reduced by 14–24% relative to present-day conditions on Twitchell Island if the entire island is converted to rice or wetlands.

4.2. Carbon dioxide

Patterns of NEE at each site followed a seasonal pattern where carbon uptake was highest during the spring and summer months (Fig. 5). Peak carbon uptake at each site corresponds to periods with high solar radiation since both the grazed degraded peatland and the rice paddy have a plant-accessible water table, preventing water limitation even though there is no rainfall during this period. Interestingly, both sites had similar annual budgets of ecosystem photosynthesis in each year (Table 3), indicating that the plant canopy at each site is well-established with similar carbon capture potentials. Since the grazed degraded peatland and rice paddy are situated in the same climate with the same incoming radiation, the same C3 photosynthetic pathway, and are both not water-limited, the main difference in plant cover type between the two sites is that the grazed degraded peatland has perennial vegetation with a lower canopy photosynthetic capacity, and the rice paddy has annual vegetation with a higher photosynthetic capacity than the grazed peatland. This trade-off between perennial plants with lower photosynthetic capacity and annual plants with higher photosynthetic capacity causes the integral of P_{eco} at each site to converge when considering the annual budget of photosynthesis at the site. Because on an annual basis P_{eco} is similar between sites, the differences in NEE are attributed to different rates of R_{eco}, supporting the hypothesis that focusing management attention on limiting R_{eco} will promote net carbon capture. The differences we observed in R_{eco} between the drained grazed degraded peatland and flooded rice paddy indicated that flooding is an effective management strategy to minimize losses of C through R_{eco} by heterotrophic respiration throughout the duration of the year, as R_{eco} at the rice paddy was consistently lower than that at the grazed degraded peatland, regardless of season (Fig. 6).

The CO_2 budget for the Sherman Island grazed degraded peatland compares relatively well with that calculated from a grazed dairy cow pasture in New Zealand, which calculated the net carbon balance (including CH_4 loss and milk loss) as source of 106.1 ± 50 g-C m^{-2} yr^{-1} (Nieveen et al., 2005). The CO_2 fluxes at Sherman Island in this study are lower than those measured and reported at other drained peatland sites on Sherman Island by Deverel and Rojstaczer (1996). For soils that ranged from 10% to 15% organic carbon, Deverel and Rojstaczer (1996) measured CO_2 flux with chambers and used $^{14}CO_2$ and $^{13}CO_2$ in gas samples (Rojstaczer and Deverel, 1993) to estimate the portion of the CO_2 flux attributable to peat oxidation. Values ranged from 700 g-C m^{-2} yr^{-1} to 1110 g-C m^{-2} yr^{-1}. A key differentiating factor is likely the depth to groundwater as Deverel and Rojstaczer (1996) measured fluxes where the depth to groundwater was typically about 1 m. Stephens et al. (1984) reported a logarithmic effect of changing groundwater depth on organic-soil subsidence rates and carbon loss.

The pattern of CO_2 fluxes at the Twitchell Island rice paddy (Fig. 4) match those from work at Japanese rice paddies, which

concluded that CO_2 fluxes decreased and CH_4 increased after flooding of the rice paddy soil (Miyata et al., 2000). The pattern of NEE throughout the growing season at the rice paddy corresponds well with other studies from Japan (Saito et al., 2005) and Texas (Campbell et al., 2001), although the magnitude of the partitioned P_{eco} and R_{eco} fluxes are much smaller in our study, presumably from the lower temperatures in the Delta compared with other sites that are more traditionally suited to rice agriculture. A two-year study at a rice paddy near Sacramento, CA using the eddy covariance method found a higher rate of CO_2 uptake than in our study (-594 g-C m^{-2} yr^{-1}) due to lower rates of R_{eco} at this site (McMillan et al., 2007). However, we expect the P_{eco} of the Twitchell Island rice paddy to increase slightly over time as the study continues and managers learn to optimize the timing of planting and harvest at this new site.

Rates of CO_2 capture at the rice paddy were slightly lower than those from a riparian cottonwood stand about 50 km east of our sites, which acted as a net sink of 310 g-C m^{-2} yr^{-1} (Kochendorfer et al., 2011). The magnitude of CO_2 uptake at the rice paddy was well below that from a restored marsh in southern California, where net primary productivity captured between 458 g-C m^{-2} yr^{-1} and 1245 g-C m^{-2} yr^{-1} as CO_2 during an eight-year study (Rocha and Goulden, 2009). However, this southern California cattail marsh also had high rates of R_{eco}, making it a net carbon source of about 700 g-C m^{-2} over five years of eddy covariance measurements (Rocha and Goulden, 2008).

The largest seasonal variation in the CO_2 fluxes from the rice paddy was driven by changes in water and canopy management. In 2010, from about mid-May to early June, weeds filled the paddy field before planting, causing huge uptake in P_{eco} and a large release of CO_2 through R_{eco}. During this weed growth event, which lasted 32 days until the weeds were removed, 160 g-C m^{-2} of CO_2 was taken by weed photosynthesis (9.5% of the rice paddy annual P_{eco} in 2010–2011) and 200 g-C m^{-2} of CO_2 was released through enhanced R_{eco} (13% of the rice paddy 2010–2011 annual R_{eco}). This can be contrasted with the fluxes from the 2009 rice growing season that did not experience weed infiltration, when fluxes during the same time period captured 64 g-C m^{-2} of CO_2 through canopy photosynthesis (4.5% of the 2009–2010 annual P_{eco} budget) and released 88 g-C m^{-2} through ecosystem respiration (6.6% of the 2009–2010 annual R_{eco} budget). While enhanced ecosystem photosynthesis and R_{eco} somewhat balance each other out in this case when considering the net release of CO_2, the weed infiltration still caused a 106% increase in NEE during the period of weed infestation (42 g-C m^{-2}) when compared with the same time period in 2009 (20 g-C m^{-2}). Higher rates of NEE due to higher rates of R_{eco} than P_{eco} during the weed infestation might be attributed to soil priming by plant exudates in the well-aerated, recently disked field (Kuzyakov et al., 2000). Although higher NEE during this time period in 2010 might have also been higher due to a larger pool of labile carbon substrates from the incorporation of the rice straw from the 2009 growing season into the soil, it nonetheless created a large spike in the pattern of CO_2 exchange at the rice paddy. These results also highlight the impact that herbicides can have on the overall carbon balance of the rice paddy by controlling the amount of aerobic respiration and photosynthesis.

Flooding and drainage at the rice paddy contributes to marked pulses in CO_2 exchange (Fig. 6). Compared with other agricultural systems, growing season respiration in rice paddies can be strongly reduced by flooding (Eugster et al., 2010), where flooding acts as a "switch" for ecosystem respiration by decreasing the habitat for aerobic microorganisms in addition to creating a barrier to gas diffusion, since diffusion through water is four orders of magnitude slower than through air. Aside from the R_{eco} pulse from the weed event in the 2010 growing season, the other pulses of R_{eco} in both years at the rice paddy are tied to flooding and drainage events. The rice paddy experiences two distinct drainage events during each year: the autumn drainage before harvest, and the spring drainage before planting. While movement of the water table recorded by the pressure transducer is rapid, the enhanced R_{eco} due to degassing during drainage typically extends over a period of 14 days. In the May 2009–April 2010 time period, the autumn drainage released 99 g-C m^{-2} over 14 days (7.4% of the annual R_{eco} budget) and the spring drainage of the same duration released 74 g-C m^{-2} (5.5% of annual R_{eco}). In the May 2010–April 2011 year, autumn drainage released 99 g-C m^{-2} as CO_2 (6.6% of annual R_{eco}). The spring drainage in the 2010–2011 time period was broken into two different events, where the first 14-day drainage event released 58 g-C m^{-2} (3.9% of annual R_{eco}) and the second released 77 g-C m^{-2} (5.1% of annual R_{eco}). This rapid loss of CO_2 upon drainage emphasizes the need for continual monitoring of CO_2 fluxes throughout the entire year, and especially during and after drainage at a seasonally flooded system like a rice paddy. Drainage events contribute significant fluxes of CO_2 from the ecosystem to the atmosphere on short timescales, and thus monitoring such events is essential for calculating accurate annual budgets of CO_2 exchange. While land managers might minimize the loss of CO_2 due to respiration by maximizing the length of flooded periods, accounting of the CO_2 loss upon drainage is essential for accurate integration of an annual CO_2 budget due to the higher magnitude drainage flux.

At the grazed degraded peatland, the surface is drained year-round, which causes extreme drying of the soil surface during the summer months, and a precipitation-induced R_{eco} pulse upon the return of the autumn rains that matches the microbial pulse response observed for other semi-arid climates (Huxman et al., 2004; Xu et al., 2004). Especially upon the first rainfall during autumn there is a large pulse in R_{eco} (Fig. 6). However, the effect of these pulses on the annual NEE budget at the grazed degraded peatland is somewhat low, as the high rates of R_{eco} year-round at the grazed degraded peatland makes the impact of the pulses less significant. The first autumn rain in 2009 caused a R_{eco} pulse that respired 5% of the annual R_{eco} budget, and the autumn rain in 2010 created a R_{eco} pulse than respired 3% of the annual budget. These rain-induced R_{eco} pulses are not observed at the rice paddy since the water table is above the surface for most of the rainy season.

The grazed degraded peatland acted as a source for CO_2 in both years, whereas the rice paddy was an atmospheric sink for CO_2 (Fig. 8). However, we emphasize that during the year following a pepperweed mowing event in spring 2008, the grazed peatland acted as a net sink for CO_2 as pepperweed grew more extensively and recovered from the harvest event (Sonnentag et al., 2011b). Despite having an atypical canopy cover of the invasive pepperweed plant, the Sherman Island grazed degraded peatland site during the two years in this study was near the mean NEE from extensively managed grasslands from an analysis of 172 non-forested EC flux tower sites (Gilmanov et al., 2010). A three-year study of a 10-year abandoned agricultural peatland in the Netherlands where the water table was maintained 10 cm below the soil surface acted as a carbon sink in each year, taking up 232–446 g-C m^{-2} yr^{-1} through NEE (Hendriks et al., 2007), which compares more closely to rates from the rice paddy than the grazed degraded peatland in our study.

We emphasize that the CO_2 budgets for the rice paddy presented in Table 3 are budgets from an atmospheric perspective, and thus do not account for the removal of carbon from the ecosystem through rice grain harvest and addition of carbon by seed planting; the amount of carbon removed from the field through harvest was 231 g m^{-2} in the 2009 growing season and was 477 g m^{-2} in the 2010 growing season, and the amount of carbon added as seed was 16.8 g m^{-2} in 2009 and 7.23 g m^{-2} in 2010. Considering these additional gains and losses of carbon, the rice paddy would lose a small amount of carbon in each year of the study, even though it acts as

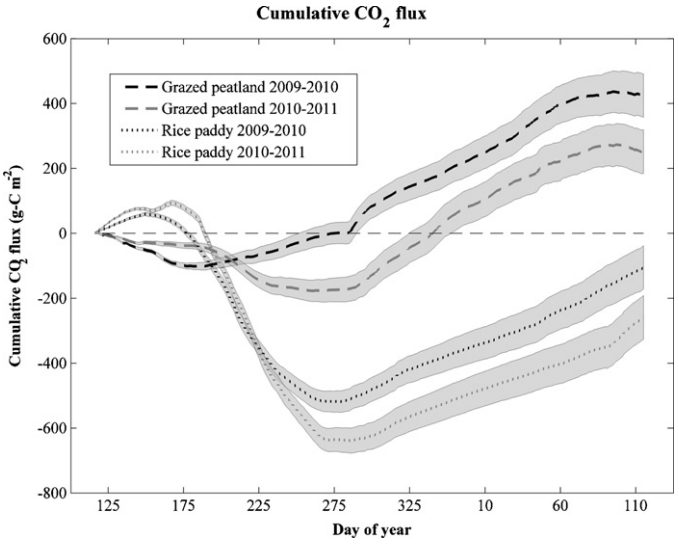

Fig. 8. Cumulative NEE. Cumulative NEE is plotted for the grazed degraded peatland (dashed lines) and rice paddy sites (dotted lines) for the two years of this study. Gray shaded areas represent the 95% confidence interval from bootstrapping the half-hourly fluxes. Due to the large uptake of CO_2 during the growing season at the rice paddy and lower rates of wintertime respiration, much less CO_2 is released to the atmosphere on an annual basis. Conversely, the lower photosynthetic CO_2 uptake and high wintertime respiration at the grazed degraded peatland make it an annual CO_2 source to the atmosphere. More favorable growing conditions in the 2010–2011 season cause greater photosynthetic uptake at both sites compared with 2009–2010.

an atmospheric sink for CO_2. Our greenhouse gas budgets also do not account for secondary emissions at either site, such as carbon footprint of electricity used to pump water or the emissions from farming machinery.

Using the partitioned annual CO_2 budgets calculated in this analysis along with soil carbon content and bulk density, it is possible to compute a "back of the envelope" approximation of the soil subsidence rates due to microbial oxidation at each of these sites. We can use the following formula to approximate soil subsidence due to soil oxidation (carbon loss) at each site:

$$\text{subsidence} = \frac{\text{NBP}}{\chi_C \rho_b}$$

where subsidence is calculated in meters, χ_C is the carbon fraction of the soil, and ρ_b is the bulk density in g m^{-3} (Table 1). NBP is net biome productivity in g-C m^{-2} yr^{-1} (Chapin et al., 2006), which at the grazed degraded peatland is equal to the sum of NEE and CH_4 flux, and at the rice paddy is equal to the carbon in harvested grain subtracted from the sum of NEE, CH_4 flux, and the carbon in seeds added. At the grazed degraded peatland, we did not account for the cattle component of NBP since we did not measure the necessary parameters to track cattle growth (Soussana et al., 2007). However, we emphasize that accounting for the cattle component of NBP at the grazed degraded peatland would create a larger net carbon loss from the ecosystem, so that our estimate of grazed degraded peatland subsidence is an imperfect but conservative calculation.

If we assume that R_{eco} originates from the soil surface at the grazed degraded peatland and use the values from the top soil layer in Table 1, we calculate subsidence of 3.7 mm in the first year of this study, and 2.2 mm in the second year. However, if we instead assume that the grazed degraded peatland R_{eco} originates from the entire unsaturated thickness and use the average bulk density of 1.02 g cm^{-3} and 0.11 for average χ_C, we calculate subsidence of 2.6 mm in the first year and 1.5 mm in the second year. The rates of subsidence at the degraded peatland in this study are slightly lower than those measured at a different site on Sherman Island by Deverel and Rojstaczer (1996) with χ_C of 0.16, which measured all subsidence (oxidation and compaction) at rates of 4.6 mm yr^{-1} and rates of subsidence due to carbon oxidation of 3.2 mm yr^{-1}. The differences between these rates are likely due to the shallower water table at the degraded pasture relative to the site where subsidence was measured by Deverel and Rojstczer (1996), which has an average water table of 1.2 m. Stephens et al. (1984) demonstrated that subsidence rates in Florida peat soils where the depth to groundwater of 1.2 m were about 2-fold larger than rates in soils where the depth to groundwater was 0.6 m. The rates of subsidence at the drained degraded peatland in this study were also lower than rates measured on Sherman Island by Deverel and Leighton (2010), which measured 5–20 mm yr^{-1} of subsidence from 1988 to 2006 at power pole foundations, which also maintained much deeper groundwater than the degraded pasture site in this study.

At the rice paddy, assuming that R_{eco} originates above 45 cm and using the average bulk density for this layer of 0.61 g cm^{-3} and χ_C of 0.23, we determined that the rice paddy subsided 1.0 mm in the first year and 1.4 mm in the second year of this study, values lower than that from the grazed degraded peatland. While the rice paddy acts as a net carbon sink from an atmospheric perspective, it still acts as a net carbon source from a subsidence perspective due to the loss of carbon through harvest. If we do not account for the loss of grain through harvest in the NBP calculation (approximating the flooded rice paddy as a non-harvested ecosystem like a wetland) we calculated rates of soil growth at 0.58 mm in the first year and 2.0 mm in the second year. Although these data were collected only a small period of time after land-use conversion, they do indicate that after two years subsidence at the rice paddy is less than that from the drained and grazed degraded peatland.

It is also useful to compare the calculated subsidence with rates from soils with similar organic carbon content with additional agricultural management practices representative of the Delta. Since subsidence rates are correlated with soil organic carbon content (Rojstaczer and Deverel, 1995; Deverel and Leighton, 2010), larger subsidence rates than estimated for the degraded peatland are expected for soils with larger organic carbon fractions and deeper depths to groundwater. Indeed, the degraded peatland pasture is atypical as most of the Delta is farmed as corn and groundwater levels are maintained and 1–1.2 m below land surface. In a corn field in Twitchell Island, an extensometer similar to the one described in Deverel and Rojstaczer (1996) has operated since 2009 in soil with 0.15 carbon content and 1.2 m water table depth. During the first 440 days of operation, we measured subsidence of 24.6 mm yr^{-1}. Consistently, on Bacon Island, Deverel and Leighton (2010) reported 22 mm yr^{-1} of subsidence from 1978 to 2006 for an average soil organic carbon content of 0.2 and water table depth of 1.2 m. In light of these data, rice cultivation represents a substantial benefit for subsidence mitigation relative to other current agricultural management practices.

4.3. Methane

The pattern and magnitude of CH_4 fluxes at the grazed degraded peatland and rice paddy in this study were markedly different (Fig. 7), due to the difference in the management controls on emission at each site. The background soil CH_4 fluxes at the grazed degraded peatland are a mixture of fluxes from high CH_4-emitting drainage ditches and much lower CH_4-emitting upland soils (Teh et al., 2011), and thus our background CH_4 flux measurements represent an averaged value for this land-use. The CH_4 fluxes for the background ecosystem flux is generally stable throughout both 2009 and 2010 and averaged 5 mg-C m^{-2} d^{-1}, with occasional fluxes of larger magnitude during the wet winter months. This pattern compares well with results of CH_4 fluxes from a heterogeneous former agricultural peatland in the Netherlands, where measurement from both eddy covariance and chambers revealed

large spatial variability of fluxes between landforms, but a relatively stable rate of averaged ecosystem CH_4 flux throughout the year (Hendriks et al., 2010). However, rates of CH_4 flux in this Dutch agricultural peatland (24–96 mg-C m^{-2} d^{-1}) were much higher than those measured from the grazed degraded peatland in our study (2.4–12 mg-C m^{-2} d^{-1}), likely due to the much lower water table at our site (50–80 cm) compared with the 10 cm water table at the Dutch peatland. The presence of cows on drained Delta peatlands is also expected to dramatically increase the CH_4 budget of these land-uses (Shaw et al., 2007). Furthermore, the budget of nitrogen greenhouse gases is unaccounted for in each of the land use types in this study, although nitrous oxide fluxes may occasionally be high from drainage ditches at the pasture (Teh et al., 2011) and during drained conditions at rice paddies (plant and soil ref Cai et al., 1997).

The CH_4 fluxes at the rice paddy were low and stable at about 10 mg-C m^{-2} d^{-1} during the first year, but demonstrated a clear seasonal pattern of growth during the 2010 rice growing season (Fig. 7). The CH_4 fluxes during the 2010 rice growing season ranged from near zero during the start of the growing season up to 40 mg-C m^{-2} d^{-1} by mid-August 2010. The magnitude and pattern of the CH_4 fluxes from the rice paddy in this study were generally smaller than those observed by other studies of CH_4 flux in rice agriculture, although they followed a similar pattern during the 2010 growing season. Early work in Davis, CA (about 55 km north of Twitchell Island, but climatically warmer than the Delta) on rice fertilized at the same rate as the rice paddy in this study calculated daytime methane fluxes in fertilized rice at 130 mg-C m^{-2} d^{-1}, although this measurement was obtained through a single chamber campaign in late summer (Cicerone and Shetter, 1981). Subsequent work at the same site in Davis demonstrated a strong seasonal pattern in CH_4 fluxes (ranging from 0.9 mg-C m^{-2} d^{-1} to 68.7 mg-C m^{-2} d^{-1}) with a peak in late summer (Cicerone et al., 1983), and mechanistic work in Italian rice fields with the same seasonal pattern (Schutz et al., 1989) demonstrated that the late summer peak is due to favorable thermodynamic conditions for methanogenesis from acetate at this time (Kruger et al., 2001). Analysis of the year-round CH_4 budget at a rice paddy near Sacramento, CA demonstrated a strong seasonal pattern that matched that of the 2010 growing season at Twitchell Island, but with much higher CH_4 fluxes than those found in our study. The CH_4 fluxes in the Sacramento rice paddy from 2002 to 2004 peaked around 400 mg-C m^{-2} d^{-1} at the middle of the growing season (McMillan et al., 2007), much lower than the peak at 20 mg-C m^{-2} d^{-1} we saw at Twitchell Island. However, we again emphasize that our analysis only includes the first two years after land conversion, so our data might represent a land-use in a state of transition after a state change.

In this study we found very low CH_4 emissions and lack of a seasonal pattern from the Twitchell Island rice paddy in 2009 compared with typical values of CH_4 fluxes from rice agriculture (Fig. 7). As other studies have demonstrated that the labile carbon released through decomposition drive carbon cycling in rice paddies (Cicerone et al., 1992; Kimura et al., 2004), and since 2009 was the first year of rice cultivation at this site, we suggest that the low emissions in 2009 were due to the lack of labile organic carbon substrate within the soil due to the past land-use history. When corn and alfalfa agriculture was practiced at Twitchell Island, all plant litter was harvested after each growing season, preventing the input of large quantities of fresh labile carbon back into the soil. So, although the soil has very high carbon content, we believe the pool of labile carbon compounds small enough to meet the metabolic needs of methanogens (Megonigal et al., 2003) were in insufficient quantity until the first harvest of rice straw was incorporated into the soil after the 2009 growing season. Following this line of reasoning, we expect to see growing amounts of CH_4 emitted from the rice paddy as more fresh rice straw is incorporated into the soil following the harvest each year, up to some maximum threshold of CH_4 production. Lagged effects of land-use change are important to investigate through multi-year studies, and investigation of CH_4 dynamics at this site is still underway to determine whether the difference in CH_4 between 2009 and 2010 is the result of interannual variability or represents a long-term trend.

In addition to gradual trends throughout the growing season, the pattern of CH_4 emissions at the Twitchell Island rice paddy also show a large release of CH_4 upon drainage of the field for harvest. This pattern matches that of other work that measured quasi-continuous fluxes of CH_4 upon drainage, and found that the drainage flux was due to a combination of degassing due to reduced hydrostatic pressure in addition to decreased methanotrophy (CH_4 oxidation) due to the more rapid transport of CH_4 through the soil profile (Han et al., 2005). Water table management also controls CH_4 fluxes at the Twitchell Island rice paddy, since anaerobic conditions for methane production only occur in saturated conditions, after the sequence of more favorable electron acceptors for anaerobic metabolism have been depleted (Megonigal et al., 2003). Evidence from studies in Asian rice agriculture has suggested that mid-season drainage of the rice paddy may mitigate annual emissions of CH_4, since a brief aerobic period may re-oxidize reduced alternative electron acceptors to again make methanogenesis energetically unfavorable upon re-flooding (Li, 2005).

5. Conclusions

The Delta has experienced extreme rates of subsidence and carbon loss due to peat oxidation, and continuing the practice of drained agriculture will likely be infeasible and unsustainable in the near future. One of the most promising interventions to halt further subsidence and to turn Delta landscapes into carbon sinks is to convert drained landscapes back to flooded conditions; however, the efficacy of this practice in the Delta remains relatively untested (but for an example in a restored wetland see Miller et al. (2008)). Rice agriculture has been proposed as a flooded agricultural land-use type that can prevent subsidence by limiting ecosystem respiration, and our study concluded that in the short-term, the Delta rice paddy was effective at capturing CO_2 from the atmosphere and acting as a net carbon sink from an atmospheric perspective. Considering the net biome productivity of the rice ecosystem and accounting for the carbon losses from harvest indicated that the rice paddy was still a net source of carbon from an ecosystem perspective. However, the rice paddy experienced subsidence rates lower than those of the grazed degraded peatland and more than an order of magnitude lower than subsidence rates of over 20 mm yr^{-1} for agricultural soils in the Delta farmed for corn. From a subsidence perspective, rice appears to provide a substantial benefit for Delta agricultural sustainability.

The flooded status of the rice paddy also had secondary effects on the greenhouse gas budget through increased CH_4 production and higher rates of evaporation. While increased evaporation might be considered a negative consequence in water-limited California, it does benefit local farmers by reducing pumping costs. Since the Delta islands constantly leak water due to their location below sea level, land managers expend large amounts of energy to pump water out of the islands and increased evaporation saves on fossil fuels required for pumping. Another secondary ecosystem service that the rice paddy provides and is absent from the grazed degraded peatland is its ability to act as habitat for migrating birds during its flooded but fallow period during the non-growing season. Assessing these trade-offs within a policy context will reveal whether or not the benefits of land-use conversion from drained to flooded agriculture outweigh the costs.

The results from two years of flux measurements at the drained grazed degraded peatland and rice paddy indicated that converting from drained to flooded agricultural practices will help to buffer

the loss of soil carbon by reducing peat oxidation in the short-term, but further research is required over a much longer timescale to determine the rate of true soil carbon sequestration. While land-use conversion to rice agriculture might be a prudent choice to abate the further loss of carbon to the atmosphere when compared with conventional drained agriculture, net soil sequestration will not be attained until all the carbon lost from the ecosystem through grain harvest can be accounted for by more carbon uptake during the year. Some strategies that land managers might employ to further reduce the loss of carbon from rice agriculture in the Delta are to maintain the flooded status of soils for as long as possible, prevent weed infestations that cause unexpectedly large amounts of CO_2 loss, and to reduce soil disturbance such as tilling that can increase aeration and promote microbial soil oxidation. Optimizing the inclusion of rice straw to promote carbon sequestration and minimize loss of CH4 might also be a management option, as CH_4 emissions have been found to be closely tied with the amount of straw left in the field (Cicerone et al., 1992). As the rice paddy site has only been farmed as such for two years, these management options represent opportunities for future action to tip the carbon balance of the Delta rice agriculture to a net carbon sink.

The difficulty in replenishing soil carbon lost due to oxidation in the drained peatlands in this study should be of special concern with respect to the rapid drainage now occurring in the tropics through the conversion of tropical peatlands to agriculture (Jauhiainen et al., 2008). While the short-term results in this study indicated that re-flooding might help to stem the rates of soil subsidence, replenishing the carbon rapidly lost during the past century of drainage is will occur over a much longer timescale. Although there are additional water losses with converting from a drained to flooded system, these environmental costs can be weighed against the benefits of net sequestration, considering the release of CH_4 and increased rates of evaporation. This analysis quantified the short-term effects of drained to flooded agricultural land-use conversion in the Delta, and further study both at these sites and at different land-use types in the Delta will reveal whether it is feasible to transform the Delta landscape into a net carbon sink.

Acknowledgements

The authors thank the Department of Water Resources of California for granting access to field sites. The authors extend many thanks to Brian Brock, Jim Casey, and the rest of the management team at Twitchell Island, and Juan Mercado and Walt at Sherman Island, the land managers without whom this work would not be possible. We also thank Alex Christensen, Marga Pretorius, and Sarah Price for assistance with laboratory work. Jaclyn Hatala thanks the National Science Foundation Graduate Fellowship Program for support during this research. This research was supported by National Science Foundation ATM grant number AGS-0628720 and the California Department of Water Resources grant #006550.

Appendix A. Supplementary data

Supplementary data associated with this article can be found, in the online version, at doi:10.1016/j.agee.2012.01.009.

References

Armentano, T.V., 1980. Drainage of organic soils as a factor in the world cabon-cycle. Bioscience 30, 825–830.

Baldocchi, D., Chen, Q., Chen, X.Y., Ma, S.Y., Miller, G., Ryu, Y., Xiao, J., Wenk, R., Battles, J., 2010. The dynamics of energy, water, and carbon fluxes in a Blue Oak (Quercus douglasii) savanna in California, USA. In: Hill, M.J., Hanan, N.P. (Eds.), Ecosystem Function in Global Savannas: Measurement and Modeling at Landscape to Global Scales. CRC/Taylor and Francis.

Baldocchi, D., Detto, M., Sonnentag, O., Verfaillie, J., in press. The challenges of measuring methane fluxes and concentrations over a peatland pasture. Agric. Forest Meteorol., doi:10.1016/j.agrformet.2011.04.013.

Baldocchi, D.D., Hicks, B.B., Meyers, T.P., 1988. Measuring biosphere–atmosphere exchanges of biologically related gases with micrometeorological methods. Ecology 69, 1331–1340.

Bianchi, T.S., Allison, M.A., 2009. Large-river delta-front estuaries as natural recorders of global environmental change. Proc. Natl. Acad. Sci. U. S. A. 106, 8085–8809.

Cai, Z.C., Xing, G.X., Yan, X.Y., Xu, H., Tsuruta, H., Yagi, K., Minami, K., 1997. Methane and nitrous oxide emissions from rice paddy fields as affected by nitrogen fertilisers and water management. Plant and Soil 196, 7–14.

Campbell, C.S., Heilman, J.L., McInnes, K.J., Wilson, L.T., Medley, J.C., Wu, C.W., Cobos, D.R., 2001. Diel and seasonal variation in CO2 flux of irrigated rice. Agric. Forest Meteorol. 108, 15–27.

Canuel, E.A., Lerberg, E.J., Dickhut, R.M., Kuehl, S.A., Bianchi, T.S., Wakeham, S.G., 2009. Changes in sediment and organic carbon accumulation in a highly-disturbed ecosystem: the Sacramento-San Joaquin River Delta (California, USA). Mar. Pollut. Bull. 59, 154–163.

Chapin III, F.S., Woodwell, G.M., Randerson, J.T., Rastetter, E.B., Lovett, G.M., Baldocchi, D.D., Clark, D.A., Harmon, M.E., Schimel, D.S., Valentini, R., Wirth, C., Aber, J.D., Cole, J.J., Goulden, M.L., Harden, J.W., Heimann, M., Howarth, R.W., Matson, P.A., McGuire, A.D., Melillo, J.M., Mooney, H.A., Neff, J.C., Houghton, R.A., Pace, M.L., Ryan, M.G., Running, S.W., Sala, O.E., Schlesinger, W.H., Schulze, E.D., 2006. Reconciling carbon-cycle concepts, terminology, and methods. Ecosystems 9, 1041–1050.

Cicerone, R.J., Delwiche, C.C., Tyler, S.C., Zimmerman, P.R., 1992. Methane emissions from California rice paddies with varied treatments. Global Biogeochem. Cycles 6, 233–248.

Cicerone, R.J., Shetter, J.D., 1981. Sources of atmospheric methane – measurements in rice paddies and a discussion. J. Geophys. Res. Oceans Atmos. 86, 7203–7209.

Cicerone, R.J., Shetter, J.D., Delwiche, C.C., 1983. Seasonal-variation of methane flux from a California rice paddy. J. Geophys. Res. Oceans Atmos. 88, 1022–1024.

Conrad, R., 2007. Microbial ecology of methanogens and methanotrophs. In: Sparks, D.L. (Ed.), Advances in Agronomy, vol. 96. Elsevier, San Francisco, pp. 1–63.

Crooks, S., 2009. The impacts of sea level rise on tidal wetlands: Implications for carbon sequestration and estuarine management. Philip Williams & Associates for the Resources Legacy Fund, San Francisco, CA.

Detto, M., Baldocchi, D., Katul, G.G., 2010. Scaling properties of biologically active scalar concentration fluctuations in the atmospheric surface layer over a managed peatland. Bound. Layer Meteorol. 136, 407–430.

Detto, M., Katul, G.G., 2007. Simplified expressions for adjusting higher-order turbulent statistics obtained from open path gas analyzers. Bound. Layer Meteorol. 122, 205–216.

Detto, M., Verfaillie, J., Anderson, F., Xu, L., Baldocchi, D., 2011. Comparing laser-based open- and closed-path gas analyzers to measure methane fluxes using the eddy covariance method. Agric. Forest Meteorol. 151, 1312–1324.

Deverel, S.J., Leighton, D.A., 2010. Historic, recent, and future subsidence, Sacramento-San Joaquin Delta, California, USA. San Francisco Estuary and Watershed Science 8.

Deverel, S.J., Leighton, D.A., Sola-Llonch, N., 2007. Appendix C: evaluation of island drain flow, seepage, and organic carbon loads, Sacramento-San Joaquin Delta. Results from the Delta Learning Laboratory Project. California Department of Water Resources and CALFED Bay Delta Authority, CALFED Project 98-C01.

Deverel, S.J., Rojstaczer, S., 1996. Subsidence of agricultural lands in the Sacramento San Joaquin Delta, California: Role of aqueous and gaseous carbon fluxes. Water Resources Research 32, 2359–2367.

Drexler, J.Z., Anderson, F.E., Snyder, R.L., 2008. Evapotranspiration rates and crop coefficients for a restored marsh in the Sacramento-San Joaquin Delta, California, USA. Hydrol. Process. 22, 725–735.

Drexler, J.Z., de Fontaine, C.S., Brown, T.A., 2009a. Peat accretion histories during the past 6,000 years in the marshes of the Sacramento-San Joaquin Delta, CA, USA. Estuaries Coasts 32, 871–892.

Drexler, J.Z., de Fontaine, C.S., Deverel, S.J., 2009b. The legacy of wetland drainage on the remaining peat in the Sacramento-San Joaquin Delta, California, USA. Wetlands 29, 372–386.

Drexler, J.Z., De Fontaine, C.S., Knifong, D.L., 2007. Age Determination of the Remaining Peat in the Sacramento-San Joaquin Delta, California, USA. United States Geological Survey, Sacramento, CA.

Eugster, W., Moffat, A.M., Ceschia, E., Aubinet, M., Ammann, C., Osborne, B., Davis, P.A., Smith, P., Jacobs, C., Moors, E., Le Dantec, V., Beziat, P., Saunders, M., Jans, W., Gruenwald, T., Rebmann, C., Kutsch, W.L., Czerny, R., Janous, D., Moureaux, C., Dufranne, D., Carrara, A., Magliulo, V., Di Tommasi, P., Olesen, J.E., Schelde, K., Olioso, A., Bernhofer, C., Cellier, P., Larmanou, E., Loubet, B., Wattenbach, M., Marloie, O., Sanz, M.-J., Sogaard, H., Buchmann, N., 2010. Management effects on European cropland respiration. Agric. Ecosyst. Environ. 139, 346–362.

Foley, J.A., DeFries, R., Asner, G.P., Barford, C., Bonan, G., Carpenter, S.R., Chapin, F.S., Coe, M.T., Daily, G.C., Gibbs, H.K., Helkowski, J.H., Holloway, T., Howard, E.A., Kucharik, C.J., Monfreda, C., Patz, J.A., Prentice, I.C., Ramankutty, N., Snyder, P.K., 2005. Global consequences of land use. Science 309, 570–574.

Forster, P., Ramaswamy, V., Artaxo, P., Berntsen, T., Betts, R.A., Fahey, D.W., Haywood, J., Lean, J., Lowe, D.C., Myhre, G., Nganga, J., Prinn, R., Raga, G., Schulz, M., Van Dorland, R., 2007. Changes in atmospheric constituents and in radiative forcing. In: Solomon, S., Qin, D., Manning, M., Chen, Z., Marquis, M., Averyt, K.B., Tignor, M., Miller, H.L. (Eds.), Climate Change 2007: The Physical Science Basis. Contribution of Working Group I to the Fourth Assessment Report of the

Intergovernmental Panel on Climate Change. Cambridge University Press, New York.
Gilmanov, T.G., Aires, L., Barcza, Z., Baron, V.S., Belelli, L., Beringer, J., Billesbach, D., Bonal, D., Bradford, J., Ceschia, E., Cook, D., Corradi, C., Frank, A., Gianelle, D., Gimeno, C., Gruenwald, T., Guo, H., Hanan, N., Haszpra, L., Heilman, J., Jacobs, A., Jones, M.B., Johnson, D.A., Kiely, G., Li, S., Magliulo, V., Moors, E., Nagy, Z., Nasyrov, M., Owensby, C., Pinter, K., Pio, C., Reichstein, M., Sanz, M.J., Scott, R., Soussana, J.F., Stoy, P.C., Svejcar, T., Tuba, Z., Zhou, G., 2010. Productivity, respiration, and light-response parameters of world grassland and agroecosystems derived from flux-tower measurements. Rangeland Ecol. Manag. 63, 16–39.
Goulden, M.L., Litvak, M., Miller, S.D., 2007. Factors that control Typha marsh evapotranspiration. Aqua. Bot. 86, 97–106.
Hagen, S.C., Braswell, B.H., Linder, E., Frolking, S., Richardson, A.D., Hollinger, D.Y., 2006. Statistical uncertainty of eddy flux-based estimates of gross ecosystem carbon exchange at Howland Forest, Maine. J. Geophys. Res. Atmos. 111, D08S03.
Han, G.H., Yoshikoshi, H., Nagai, H., Yamada, T., Saito, M., Miyata, A., Harazono, Y., 2005. Concentration and carbon isotope profiles of CH4 in paddy rice canopy: Isotopic evidence for changes in CH4 emission pathways upon drainage. Chem. Geol. 218, 25–40.
Harazono, Y., Kim, J., Miyata, A., Choi, T., Yun, J.I., Kim, J.W., 1998. Measurement of energy budget components during the International Rice Experiment (IREX) in Japan. Hydrol. Process. 12, 2081–2092.
Hendriks, D.M.D., van Huissteden, J., Dolman, A.J., 2010. Multi-technique assessment of spatial and temporal variability of methane fluxes in a peat meadow. Agric. Forest Meteorol. 150, 757–774.
Hendriks, D.M.D., van Huissteden, J., Dolman, A.J., van der Molen, M.K., 2007. The full greenhouse gas balance of an abandoned peat meadow. Biogeosciences 4, 411–424.
Hoffman, G.J., Maas, E.V., Prichard, T.L., Meyer, J.L., 1983. Salt tolerance of corn in the Sacramento-San Joaquin Delta of California. Irrig. Sci. 4, 31–44.
Holzapfel-Pschorn, A., Conrad, R., Seiler, W., 1986. Effects of vegetation on the emission of methane from submerged paddy soil. Plant Soil 92, 223–233.
Huxman, T.E., Snyder, K.A., Tissue, D., Leffler, A.J., Ogle, K., Pockman, W.T., Sandquist, D.R., Potts, D.L., Schwinning, S., 2004. Precipitation pulses and carbon fluxes in semiarid and arid ecosystems. Oecologia 141, 254–268.
Jans, W.W.P., Jacobs, C.M.J., Kruijt, B., Elbers, J.A., Barendse, S., Moors, E.J., 2010. Carbon exchange of a maize (*Zea mays* L.) crop: Influence of phenology. Agric. Ecosyst. Environ. 139, 316–324.
Jauhiainen, J., Limin, S., Silvennoinen, H., Vasander, H., 2008. Carbon dioxide and methane fluxes in drained tropical peat before and after hydrological restoration. Ecology 89, 3503–3514.
Kaimal, J.C., Gaynor, J.E., 1991. Another look at sonic thermometry. Bound. Layer Meteorol. 56, 401–410.
Kimura, M., Murase, J., Lu, Y.H., 2004. Carbon cycling in rice field ecosystems in the context of input, decomposition and translocation of organic materials and the fates of their end products (CO_2 and CH_4). Soil Biol. Biochem. 36, 1399–1416.
Kochendorfer, J., Castillo, E.G., Haas, E., Oechel, W.C., Paw, U.K.T., 2011. Net ecosystem exchange, evapotranspiration and canopy conductance in a riparian forest. Agric. Forest Meteorol. 151, 544–553.
Kruger, M., Frenzel, P., Conrad, R., 2001. Microbial processes influencing methane emission from rice fields. Global Change Biol. 7, 49–63.
Kuzyakov, Y., Friedel, J.K., Stahr, K., 2000. Review of mechanisms and quantification of priming effects. Soil Biol. Biochem. 32, 1485–1498.
Li, C., 2005. Modeling impacts of farming management alternatives on CO2, CH4, and N2O emissions: A case study for water management of rice agriculture of China. Global Biogeochem. Cycles 19, GB3010.
Lourence, F.J., Pruitt, W.O., 1971. Energy balance and water use of rice grown in the Central Valley of California. Agron. J. 63, 827–832.
Lund, J., Hanak, E., Fleenor, W., Howitt, R., Mount, J., Moyle, P., 2007. Envisioning Futures for the Sacramento-San Joaquin Delta. Public Policy Institute of California, San Francisco, CA.
Massman, W.J., Lee, X., 2002. Eddy covariance flux corrections and uncertainties in long-term studies of carbon and energy exchanges. Agric. Forest Meteorol. 113, 121–144.
McMillan, A.M.S., Goulden, M.L., Tyler, S.C., 2007. Stoichiometry of CH4 and CO2 flux in a California rice paddy. J. Geophys. Res. 112, G01008.
Megonigal, J.P., Hines, M.E., Visscher, P.T., 2003. Anaerobic metabolism: linkages to trace gases and aerobic processes. In: Schlesinger, W.H. (Ed.), Biogeochemistry. Elsevier, New York, NY, pp. 319–424.
Miller, R.L., Fram, M., Fujii, R., Wheeler, G., 2008. Subsidence reversal in a re-established wetland in the Sacramento-San Joaquin Delta, California, USA. San Francisco Estuary and Watershed Science, 6.
Miller, R.L., Hastings, L., Fujii, R., 2000. Hydrologic treatments affect gaseous carbon loss from organic soils, Twitchell Island, California, October 1995–December 1997. U. S. Geological Survey Water Resources Investigations Report 00-4042.
Miyata, A., Leuning, R., Denmead, O.T., Kim, J., Harazono, Y., 2000. Carbon dioxide and methane fluxes from an intermittently flooded paddy field. Agric. Forest Meteorol. 102, 287–303.
Mount, J., Twiss, R., 2005. Subsidence, sea level rise, and seismicity in the Sacramento-San Joaquin Delta. San Francisco Estuary and Watershed Science 3, Article 5.
Nieveen, J.P., Campbell, D.I., Schipper, L.A., Blair, I.J., 2005. Carbon exchange of grazed pasture on a drained peat soil. Global Change Biol. 11, 607–618.
Papale, D., Reichstein, M., Aubinet, M., Canfora, E., Bernhofer, C., Kutsch, W., Longdoz, B., Rambal, S., Valentini, R., Vesala, T., Yakir, D., 2006. Towards a standardized processing of Net Ecosystem Exchange measured with eddy covariance technique: algorithms and uncertainty estimation. Biogeosciences 3, 571–583.
Papale, D., Valentini, A., 2003. A new assessment of European forests carbon exchanges by eddy fluxes and artificial neural network spatialization. Global Change Biol. 9, 525–535.
Penman, H.L., 1948. Natural evaporation from open water, bare soil and grass. Proceedings of the Royal Society of London Series a-Mathematical and Physical Sciences 193, 120–145.
Pielke, R.A., Marland, G., Betts, R.A., Chase, T.N., Eastman, J.L., Niles, J.O., Niyogi, D.D.S., Running, S.W., 2002. The influence of land-use change and landscape dynamics on the climate system: relevance to climate-change policy beyond the radiative effect of greenhouse gases. Philos. Trans. R. Soc. Lond. Ser. A-Math. Phys. Eng. Sci. 360, 1705–1719.
Pruitt, W.O., Lourence, F.J., von Oettinger, S., 1972. Water use by crops as affected by climate and plant factors. California Agric. 26, 10–14.
Ramankutty, N., Evan, A.T., Monfreda, C., Foley, J.A., 2008. Farming the planet: 1. Geographic distribution of global agricultural lands in the year 2000. Global Biogeochem. Cycles 22, GB1003.
Reichstein, M., Falge, E., Baldocchi, D., Papale, D., Aubinet, M., Berbigier, P., Bernhofer, C., Buchmann, N., Gilmanov, T., Granier, A., Grunwald, T., Havrankova, K., Ilvesniemi, H., Janous, D., Knohl, A., Laurila, T., Lohila, A., Loustau, D., Matteucci, G., Meyers, T., Miglietta, F., Ourcival, J.M., Pumpanen, J., Rambal, S., Rotenberg, E., Sanz, M., Tenhunen, J., Seufert, G., Vaccari, F., Vesala, T., Yakir, D., Valentini, R., 2005. On the separation of net ecosystem exchange into assimilation and ecosystem respiration: review and improved algorithm. Global Change Biol. 11, 1424–1439.
Rinne, J., Riutta, T., Pihlatie, M., Aurela, M., Haapanala, S., Tuovinen, J.-P., Tuittila, E.-S., Vesala, T., 2007. Annual cycle of methane emission from a boreal fen measured by the eddy covariance technique. Tellus B 59, 449–457.
Rocha, A.V., Goulden, M.L., 2008. Large interannual CO(2) and energy exchange variability in a freshwater marsh under consistent environmental conditions. J. Geophys. Res. Biogeosci. 113, G03026.
Rocha, A.V., Goulden, M.L., 2009. Why is marsh productivity so high? New insights from eddy covariance and biomass measurements in a Typha marsh. Agric. Forest Meteorol. 149, 159–168.
Rojstaczer, S., Deverel, S.J., 1993. Time-dependence in atmospheric carbon inputs from drainage of organic soils. Geophys. Res. Lett. 20, 1383–1386.
Rojstaczer, S., Deverel, S.J., 1995. Land subsidence in drained histosols and highly organic mineral soils of California. Soil Sci. Soc. Am. J. 59, 1162–1167.
Ryu, Y., Baldocchi, D.D., Ma, S., Hehn, T., 2008. Interannual variability of evapotranspiration and energy exchange over an annual grassland in California. J. Geophys. Res. Atmos. 113, D09104.
Saito, M., Miyata, A., Nagai, H., Yamada, T., 2005. Seasonal variation of carbon dioxide exchange in rice paddy field in Japan. Agric. Forest Meteorol. 135, 93–109.
Schotanus, P., Nieuwstadt, F.T.M., Debruin, H.A.R., 1983. Temperature measurement with a sonic anemometer and its application to heat and moisture fluxes. Bound. Layer Meteorol. 26, 81–93.
Schutz, H., Seiler, W., Conrad, R., 1989. Processes involved in formation and emission of methane in rice paddies. Biogeochemistry 7, 33–53.
Schwarzenegger, A., Isenberg, P., Florian, M., Frank, R., McKernan, T., McPeak, S., Reilly, W., Seed, R., 2008. Delta Vision Strategic Plan. State of California Resources Agency, Sacramento.
Shaw, S.L., Mitloehner, F.M., Jackson, W., Depeters, E.J., Fadel, J.G., Robinson, P.H., Holzinger, R., Goldstein, A.H., 2007. Volatile organic compound emissions from dairy cows and their waste as measured by proton-transfer-reaction mass spectrometry. Environ. Sci. Technol. 41, 1310–1316.
Shlemon, R.J., Begg, E.L., 1975. Late Quaternary evolution of the Sacramento-San Joaquin Delta, California. Quat. Stud. 13, 259–266.
Shuttleworth, W.J., 2007. Putting the 'vap' into evaporation. Hydrol. Earth Syst. Sci. 11, 210–244.
Smith, P., Martino, D., Cai, Z., Gwary, D., Janzen, H., Kumar, P., McCarl, B., Ogle, S., O'Mara, F., Rice, C., Scholes, B., Sirotenko, O., 2007. Agriculture. In: Metz, B., Davidson, O.R., Bosch, P.R., Dave, R., Meyer, L.A. (Eds.), Climate Change 2007: Mitigation. Contribution of Working Group III to the Fourth Assessment Report of the Intergovernmental Panel on Climate Change. Cambridge University Press, Cambridge, UK and New York, NY.
Sonnentag, O., Detto, M., Runkle, B.R.K., Teh, Y.A., Silver, W.L., Kelly, M., Baldocchi, D.D., 2011. Carbon dioxide exchange of a pepperweed (*Lepidium latifolium* L.) infestation: How do flowering and mowing affect canopy photosynthesis and autotrophic respiration? J. Geophys. Res. 116, G01021.
Sonnentag, O., Detto, M., Vargas, R., Ryu, Y., Runkle, B.R.K., Kelly, M., Baldocchi, D.D., 2011. Tracking the structural and functional development of a perennial pepperweed (*Lepidium latifolium* L.) infestation using a multi-year archive of webcam imagery and eddy covariance measurements. Agric. Forest Meteorol. 151, 916–926.
Soussana, J.F., Allard, V., Pilegaard, K., Ambus, P., Amman, C., Campbell, C., Ceschia, E., Clifton-Brown, J., Czobel, S., Domingues, R., Flechard, C., Fuhrer, J., Hensen, A., Horvath, L., Jones, M., Kasper, G., Martin, C., Nagy, Z., Neftel, A., Raschi, A., Baronti, S., Rees, R.M., Skiba, U., Stefani, P., Manca, G., Sutton, M., Tubaf, Z., Valentini, R., 2007. Full accounting of the greenhouse gas (CO2, N2O, CH4) budget of nine European grassland sites. Agric. Ecosyst. Environ. 121, 121–134.
Stephens, J.C., Allen, L.H., Chen, E., 1984. Organic soil subsidence. In: Holzer, T.L. (Ed.), Man-Induced Land Subsidece. Reviews in Engineering Geology. Geological Society of America, Boulder, CO.

Syvitski, J.P.M., Kettner, A.J., Overeem, I., Hutton, E.W.H., Hannon, M.T., Brakenridge, G.R., Day, J., Vorosmarty, C., Saito, Y., Giosan, L., Nicholls, R.J., 2009. Sinking deltas due to human activities. Nat. Geosci. 2, 681–686.

Teh, Y.A., Silver, W.L., Conrad, M.E., 2005. Oxygen effects on methane production and oxidation in humid tropical forest soils. Global Change Biol. 11, 1283–1297.

Teh, Y.A., Silver, W.L., Sonnentag, O., Detto, M., Kelly, M., Baldocchi, D.D., 2011. Large greenhouse gas emissions from a temperate peatland pasture. Ecosystems 14, 311–325.

Thompson, J., 1957. The settlement geography of the Sacramento-San Joaquin Delta, California. Geography. Stanford University, Palo Alto, p. 660.

Tyler, S.C., Bilek, R.S., Sass, R.L., Fisher, F.M., 1997. Methane oxidation and pathways of production in a Texas paddy field deduced from measurements of flux, delta C-13, and delta D of CH4. Global Biogeochem. Cycles 11, 323–348.

Uchijima, Z., 1976. Maize and Rice. In: Monteith, J. (Ed.), Vegetation and the Atmosphere. Academic Press Inc., New York, NY.

van Gorsel, E., Delpierre, N., Leuning, R., Black, A., Munger, J.W., Wofsy, S., Aubinet, M., Feigenwinter, C., Beringer, J., Bonal, D., Chen, B., Chen, J., Clement, R., Davis, K.J., Desai, A.R., Dragoni, D., Etzold, S., Gruenwald, T., Gu, L., Heinesch, B., Hutyra, L.R., Jans, W.W.P., Kutsch, W., Law, B.E., Leclerc, M.Y., Mammarella, I., Montagnani, L., Noormets, A., Rebmann, C., Wharton, S., 2009. Estimating nocturnal ecosystem respiration from the vertical turbulent flux and change in storage of CO(2). Agric. Forest Meteorol. 149, 1919–1930.

Waddington, J.M., Strack, M., Greenwood, M.J., 2010. Toward restoring the net carbon sink function of degraded peatlands: Short-term response in CO2 exchange to ecosystem-scale restoration. J. Geophys. Res. Biogeosci. 115, G04044.

Webb, E.K., Pearman, G.I., Leuning, R., 1980. Correction of flux measurements for density effects due to heat and water-vapor transfer. Quart. J. R. Meteorol. Soc. 106, 85–100.

Weir, W.W., 1950. Subsidence of peat lands of the Sacramento-San Joaquin Delta, California. Hilgardia 20, 37–56.

Wilson, K., Goldstein, A., Falge, E., Aubinet, M., Baldocchi, D., Berbigier, P., Bernhofer, C., Ceulemans, R., Dolman, H., Field, C., Grelle, A., Ibrom, A., Law, B.E., Kowalski, A., Meyers, T., Moncrieff, J., Monson, R., Oechel, W., Tenhunen, J., Valentini, R., Verma, S., 2002. Energy balance closure at FLUXNET sites. Agric. Forest Meteorol. 113, 223–243.

Worrall, F., Bell, M.J., Bhogal, A., 2010. Assessing the probability of carbon and greenhouse gas benefit from the management of peat soils. Sci. Total Environ. 408, 2657–2666.

Xu, L.K., Baldocchi, D.D., Tang, J.W., 2004. How soil moisture, rain pulses, and growth alter the response of ecosystem respiration to temperature. Global Biogeochem. Cycles 18, GB4002.